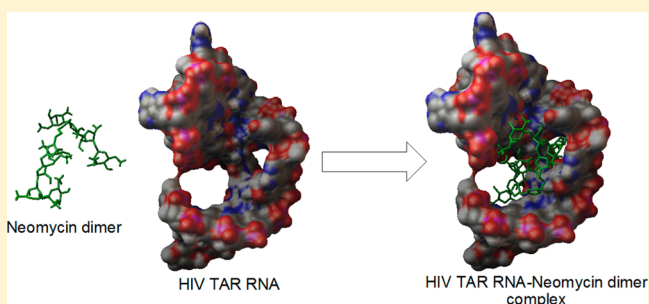


Click Dimers To Target HIV TAR RNA Conformation

Sunil Kumar,[†] Patrick Kellish,[†] W. Edward Robinson, Jr.,[‡] Deyun Wang,[§] Daniel H. Appella,[§] and Dev P. Arya^{*†}[†]Laboratory of Medicinal Chemistry, Department of Chemistry, Clemson University, Clemson, South Carolina 29634, United States[‡]Department of Pathology and Laboratory Medicine, University of California, Irvine, California 92697, United States[§]Laboratory of Bioorganic Chemistry, National Institute of Diabetes and Digestive and Kidney Diseases, National Institutes of Health, Bethesda, Maryland 20892, United States

Supporting Information

ABSTRACT: A series of neomycin dimers have been synthesized using “click chemistry” with varying functionality and length in the linker region to target the human immunodeficiency virus type 1 (HIV-1) TAR RNA region of the HIV virus. The TAR (Trans-Activation Responsive) RNA region, a 59 bp stem–loop structure located at the 5′-end of all nascent viral transcripts, interacts with its target, a key regulatory protein, Tat, and necessitates the replication of HIV-1. Neomycin, an aminosugar, has been shown to exhibit multiple binding sites on TAR RNA. This observation prompted us to design and synthesize a library of triazole-linked neomycin dimers using click chemistry. The binding between neomycin dimers and TAR RNA was characterized using spectroscopic techniques, including FID (fluorescent intercalator displacement), a FRET (fluorescence resonance energy transfer) competitive assay, circular dichroism (CD), and UV thermal denaturation. UV thermal denaturation studies demonstrate that binding of neomycin dimers increases the melting temperature (T_m) of the HIV TAR RNA up to 10 °C. Ethidium bromide displacement (FID) and a FRET competition assay revealed nanomolar binding affinity between neomycin dimers and HIV TAR RNA, while in case of neomycin, only weak binding was detected. More importantly, most of the dimers exhibited lower IC_{50} values toward HIV TAR RNA, when compared to the fluorescent Tat peptide, and show increased selectivity over mutant TAR RNA. Cytopathic effects investigated using MT-2 cells indicate a number of the dimers with high affinity toward TAR show promising anti-HIV activity.



Ribonucleic acid–protein interactions are essential for regulation of many important biological processes such as translation, RNA splicing, and transcription.^{1–3} An important example of such an interaction is involved in the regulation of human immunodeficiency virus type 1 (HIV-1). HIV TAR RNA (trans-activation responsive region), a 59 bp stem–loop structure located at the 5′-end of the nascent viral transcripts, interacts with Tat protein (an 86-amino acid protein) and regulates the level of transcription of HIV.^{4,5} The cooperative interaction of Tat protein along with its cellular cofactor, transactivating elongation factor-b (TEFb), with TAR RNA recruits and activates the CDK9 kinase that phosphorylates RNA polymerase II (RNAP II) and significantly enhances the processivity of RNAP II.^{3,6,7}

HIV transcription in virus-infected cells is strongly triggered by the interaction between Tat protein and its cognate TAR RNA. TAR RNA structure is comprised of two stems (upper and lower), a three-nucleotide bulge region, and a hairpin. An arginine rich domain of Tat protein interacts with the trinucleotide bulge (U23, C24, and U25) of TAR RNA^{1,8,9} and causes a substantial enhancement in the transcript level (~100-fold).² Nuclear magnetic resonance (NMR) studies show that the complexation takes place specifically between the arginine residue of

Tat protein and a guanine base in the major groove of TAR RNA.¹⁰ Disruption of the TAR RNA–Tat interaction therefore represents an attractive strategy for inhibiting viral replication. A number of molecules have been investigated with this strategy in mind.^{11,12} These include intercalators¹² (ethidium bromide¹³ and proflavine), DNA minor groove binders¹⁴ (Hoechst 33258 and DAPI), phenothiazine,¹⁵ argininamide,¹⁶ peptides,¹⁷ peptidomimetics,¹⁸ aminoglycosides,¹⁹ and cyclic polypeptides.²⁰

Aminoglycosides are naturally occurring aminosugars that bind to a wide variety of RNA structures.²¹ In the past few years, a number of aminoglycoside conjugates have been synthesized to achieve higher binding affinity and specificity toward RNA^{21–26} and DNA-based targets^{27–44} such as duplex,⁴⁵ triplex,^{46–48} and quadruplex structures.^{29,30} In an attempt to achieve higher binding affinity and explore multiple binding sites on RNA targets, the homo- and heterodimeric units of aminoglycosides^{49,50} (tobramycin, neamine, neomycin B, and kanamycin A) have been synthesized with various linker lengths and functionalities through disulfide bond formation.

Received: November 2, 2011

Revised: February 10, 2012

Published: February 17, 2012

These aminoglycosides exhibit higher binding affinity toward the dimerized A-site 16S construct, RRE RNA, than their corresponding monomeric aminoglycoside units. Also, aminoglycoside dimers exhibit 20–12000-fold stronger inhibitory effects toward the catalytic function of the *Tetrahymena* ribozyme than the monomeric units.⁵⁰ Neamine dimers have been shown to exhibit remarkable antibiotic effects and resistance to aminoglycoside-modifying enzymes.⁵¹

Among all the aminoglycosides targeted toward TAR binding, neomycin has exhibited the strongest inhibitory effect ($<1 \mu\text{M}$).¹⁹ Electrospray ionization mass spectrometry (ESI-MS)⁵² and ribonuclease protection experiments²² have suggested that the binding site of neomycin is the stem region just below the trinucleotide bulge in TAR RNA. Further ESI-MS experiments and gel shift assays have revealed the existence of three neomycin binding sites on HIV TAR RNA.⁵² These sites do not overlap with the Tat binding site, and thus, neomycin shows a weak ability to allosterically compete with protein binding, leading to weak HIV inhibition. To achieve improved binding and specificity profiles, we have explored neomycin's multiple binding sites on HIV TAR RNA and designed a series of neomycin dimers using click chemistry. Even though these dimers are not expected to directly compete with Tat binding, their binding is expected to lock the conformation of RNA such that Tat–TAR binding is weakened through an allosteric mechanism. We synthesized neomycin dimers using click chemistry with various linker lengths and functionalities to optimize the RNA binding affinity. Our results show that neomycin dimers display nanomolar affinity for HIV TAR RNA. Spectroscopic techniques, UV thermal denaturation, a FID (fluorescent intercalator displacement) assay, and a FRET (fluorescence resonance energy transfer) assay were utilized to study the binding between neomycin dimers and TAR RNA. In this report, we present our work detailing a simple and efficient route toward the synthesis of triazole-linked aminosugar dimers, their binding to TAR RNA, their ability to effectively inhibit the tat–TAR interaction, and their cytopathic effects on HIV in MT-2 cells.

■ EXPERIMENTAL PROCEDURES

Materials. All of the chemicals were purchased from commercial suppliers and used without further purification. Neomycin B trisulfate was purchased from MP Biomedicals (Solon, OH). Di-*tert*-butyl dicarbonate (Boc anhydride) was purchased from Advanced ChemTech (Louisville, KY). SC (sodium cacodylate), EDTA (ethylenediaminetetraacetic acid), KCl, and sodium phosphate (mono and di) salts were purchased from Fisher Scientific. TPS-Cl (2,4,6-triisopropylbenzenesulfonyl chloride) and 4 M HCl/dioxane were purchased from Sigma Aldrich. Silica gel for flash column chromatography was purchased from Sorbent Technologies (Atlanta, GA) as silica gel standard grade (particle size of 40–63 μm). All solvents were purchased from VWR. Reaction solvents were distilled over calcium hydride [toluene, pyridine, and DCM (dichloromethane)]. EtOH (ethanol) was first distilled with sodium metal and then redistilled over magnesium turnings. Reactions were conducted under N_2 using dry solvent, unless otherwise noted.

Instrumentation. ^1H NMR spectra were recorded on a Bruker 500 MHz FT-NMR spectrometer. MS [matrix-assisted laser desorption ionization time-of-flight (MALDI-TOF)] spectra were recorded using a Bruker Omnixflex MALDI-TOF mass spectrometer. All UV spectra were recorded on a Cary 100 Bio UV–vis spectrophotometer equipped with a thermoelectrically controlled 12-cell holder. Quartz cells with a 1 cm

path length were used for all the absorbance studies. Spectrophotometer stability and λ alignment were checked prior to initiation of each melting point experiment. Fluorescence spectra were recorded on a Photon Technology International instrument (Lawrenceville, NJ). The fluorescence measurements in 96-well plates were taken on a Genios Multi-Detection Microplate Reader, TECAN, with Magellan software.

UV Thermal Denaturation Experiment. The UV thermal denaturation samples (1 mL) of TAR RNA (1 μM /strand) were mixed with a ligand (neomycin dimers) with r_{dr} values of 1 and 2 (r_{dr} is the ratio of drug to HIV TAR RNA concentration) in 100 mM KCl, 10 mM SC, and 0.5 mM EDTA (pH 6.8) and incubated for 4 h at 4 °C before the experiment was started. The UV thermal denaturation spectra of the samples in 1 cm path length quartz cuvettes were recorded at 260 nm as a function of temperature (10–95 °C, heating rate of 0.3 °C/min). First-derivative plots were used to determine the denaturation temperature.

TAR RNA Synthesis. HIV TAR RNA was purchased from Amersham Biosciences (now GE Healthcare Life Sciences, Piscataway, NJ). Before being used, HIV TAR RNA (5'-GGC AGA UCU GAG CCU GGG AGC UCU CUG CC-3') in a 10 μM batch in sterile water was heated to 95 °C for 4.5 min and then cooled rapidly in an ice bath for 5 min. This snap-cooling causes the RNA to adopt the kinetically favored hairpin rather than the thermodynamically favored duplexes.

FRET-Mediated Competition Binding Assay. The relative affinity of each dimer for HIV-1 TAR RNA was determined using a FRET-based competitive binding assay with a fluorescein-labeled HIV-1 Tat peptide as described previously.⁵³ The fluorescence experiments were performed with a Spectra Max fluorimeter (Molecular Devices) at 25 °C, with excitation and emission wavelengths of 495 and 570 nm, respectively. All samples were prepared in 96-well plates in 1 \times TK buffer [50 mM Tris and 20 mM KCl (pH 7.4)] with 0.1% Triton X-100 (Sigma). The binding affinity (IC_{50}) values reported for each dimer are the averages of three to five individual measurements and were determined by fitting the experimental data to a sigmoidal dose–response nonlinear regression model on GraphPad Prism 4.0. Prior to the competition experiments, the affinity of the fluorescein-labeled Tat peptide for HIV-1 TAR RNA was determined by monitoring fluorescence intensity changes of the fluorescent probe upon addition of HIV-1 TAR RNA. Addition of an increasing concentration (from 0 to 1000 nM) of HIV-1 TAR RNA to a 100 nM solution of fluorescein-labeled Tat peptide in TK buffer at 25 °C afforded a saturation binding curve. The IC_{50} value obtained from this binding curve was 86 nM.

Competition FRET Assay. To a solution of 100 nM HIV-1 TAR RNA and 100 nM fluorescein-labeled HIV-1 Tat peptide were added appropriate concentrations (0 nM to 100 μM) of the dimer antagonists at 25 °C; the total volume of the incubation solution was 80 μL . After 60 min, fluorescence changes of the sample solution were determined with the Spectra Max fluorimeter detector. The experimental dose–response data for a given polyamine were fit to a sigmoidal dose–response nonlinear regression model on GraphPad Prism 4.0 to afford the IC_{50} values for each dimer.

Ethidium Bromide Displacement Titration. A solution of ethidium bromide (1.25 μM , 1800 μL) was excited at 545 nm, and its fluorescence emission was monitored from 560 to 620 nm before and after the addition of HIV TAR RNA. The concentration of HIV TAR RNA was 50 nM/strand. A small

fraction of ethidium bromide is bound (<20%) under these conditions. Buffer conditions were 100 mM KCl, 10 mM SC, and 0.5 mM EDTA (pH 6.8).

Ethidium Bromide Displacement Titration To Determine the Binding Constant via Scatchard Analysis.

A solution of ethidium bromide (5.00 μ M, 1800 μ L) was excited at 545 nm, and its fluorescence emission was monitored from 560 to 620 nm before and after the addition of HIV TAR RNA. The concentration of HIV TAR RNA was 200 nM/strand. A small fraction of ethidium bromide is bound (<20%) under these conditions. Buffer conditions were 100 mM KCl, 10 mM SC, and 0.5 mM EDTA (pH 6.8).

Assay for Inhibition Activity toward HIV Antigen Synthesis in Treated Cells. Cells (500000) were pretreated with each compound for 1 h. Next, cells were inoculated with approximately 50000 infectious particles of NL4-3 (an infectious molecular clone of HIV). Infections were performed in triplicate. Every 2 days cells were pooled and stained for HIV antigen synthesis using an antibody to all HIV antigens (HIV immune globulin).

In Vitro Cell Culture To Determine the Amount of Reverse Transcriptase (RT) Activity Release. Culture supernatants were precipitated for RT release. In all assays, MT-2 cells were used, which are highly susceptible to HIV and are completely lysed by HIV. Anti-HIV activities can be routinely checked by measuring the percentage of cells positive for HIV antigens using an immunofluorescence assay (IFA) and for the release of pelletable reverse transcriptase (RT) into the supernatant. For these assays, 500000 MT-2 cells in 1 mL of medium were added to the wells of a 24-well tissue culture plate. Next, 0.5 mL of 4 \times concentrated compound was added to triplicate wells of the plate. The cells and compounds were incubated for 1 h at 37 $^{\circ}$ C. Finally, 0.5 mL of HIV_{NL4-3} produced in H9 cells (a CD4+ lymphoblastoid cell line), 100000 cpm of RT activity per well, was added to each well. Virus control wells contained no compounds. This inoculum is at a multiplicity of infection of <1. On days 2, 4, and 6, 0.75 mL of supernatants was removed and placed into individual microfuge tubes for the RT assay. The supernatants from each well were precipitated at 4 $^{\circ}$ C overnight in a solution that included 30% polyethylene glycol. After precipitation, the precipitate was lysed in a solution containing Triton X-100, Tris buffer, and DTT. The RT activity of each aliquot was determined as incorporation of [³H]dTTP into a poly(rA)-oligo(dT) template. After a 1 h assay at 37 $^{\circ}$ C, the incorporated dTTP was precipitated onto a ZetaProbe (BioRad) membrane. Slots were excised and placed into liquid scintillation cocktail. After overnight incubation, the counts per minute for each sample were determined on a β counter. Results were calculated as counts per minute per milliliter of original culture supernatant. Next, cells were resuspended in the medium, and 0.5 mL of the total remaining volume was removed for IFA. Cells were combined from their triplicate infections and pelleted, and the enriched cells were air-dried onto glass slides. The dried cells were fixed in an acetone/methanol mixture (50:50). After being fixed, cells were stained with HIV immunoglobulin, washed in PBS, and counterstained with FITC-conjugated goat and human IgG. Slides were washed in PBS, and the percentage of HIV-positive cells was determined by epifluorescence. To the remaining cells in culture was added 1.25 mL of medium, and the cultures were maintained at 37 $^{\circ}$ C.

Synthesis and Characterization of DPA51–DPA65 Dimers. *General Procedure for the Synthesis of N-Boc DPA51–DPA65.* To a solution of neomycin-Boc-5'-azide

(0.05 mmol) in dry toluene (5 mL) was added dialkyne linker (0.025 mmol, 0.50 equiv) followed by the addition of CuI (4.76 mg, 0.025 mmol) and DIPEA (6.46 mg, 0.05 mmol). The reaction mixture was stirred at 90 $^{\circ}$ C for 18 h in an atmosphere of argon. The progress of the reaction was monitored by TLC. The volatiles were rotoevaporated in vacuo. Purification by flash column chromatography (R_f = 0.38–0.44, 0 to 10% ethanol in CH₂Cl₂) afforded the desired product(s) as a white solid (percent yields are reported for individual compounds in Table 1) [R_f = 0.38–0.44, 10% ethanol in CH₂Cl₂ (v/v)].

General Procedure for the Deprotection of N-Boc DPA51–DPA65. To a solution of neomycin dimer (0.012 mmol) in dioxane (3 mL) was added a 4 M HCl/dioxane solution (1 mL), and the mixture was stirred at room temperature. A white precipitate formed after 15 min. The reaction mixture was centrifuged and the solid collected. The solid was washed with a diethyl ether/hexane solution [3 \times 5 mL, 1:1 (v/v)]. The solid was dissolved in water and lyophilized to afford the desired product(s) as a powder (percent yields are reported for individual compounds in Table 1).

DPA51: IR (neat, cm⁻¹) 3421 (br, OH), 1686, 1524, 1366; ¹H NMR (500 MHz, D₂O) δ 8.02 (s, 2 H, triazole), 5.92 (d, J = 3.94 Hz, 2 H, H_{1II}), 5.28 (d, J = 3.16 Hz, 2 H, H_{1III}), 5.17 (s, 2 H, H_{1IV}), 4.41 (m, 2 H, H_{4III}), 4.34 (d, J = 5.20 Hz, 2 H, H_{2III}), 4.18 (t, J = 4.73 Hz, 2 H, H_{4IV}), 4.10 (d, J = 2.84 Hz, 2 H, H_{4I}), 3.96 (t, J = 9.62 Hz, 2 H, H_{6II}), 3.90 (t, J = 9.93 Hz, 2 H, H_{5I}), 3.86–3.76 (m, 8 H, H_{2IV}, H_{4IV}, H_{5IV}, H_{3III}), 3.70 (d, J = 1.89 Hz, 2 H, H_{6I}), 3.54 (t, J = 9.61 Hz, 2 H, H_{3II}), 3.49–3.45 (m, 4 H, H_{3I}, H_{5II}), 3.44–3.32 (m, 2 H, H_{1I}), 3.30–3.20 (m, 8 H, H_{5III} and propargyl ether protons), 2.39–2.32 (dt, J_1 = 3.94 Hz, J_2 = 4.25 Hz, 2 H, H_{2Ieq}), 1.72–1.82 (q, J = 12.45 Hz, 2 H, H_{2Iax}); ¹³C NMR (125 MHz, D₂O) δ 162–162 (q, CF₃-COOH), 127, 125, 115, 110, 95, 85, 79, 77, 75, 73, 72, 70, 69, 68, 67, 63, 62, 53, 52, 50, 49, 48, 40.5, 40.1, 28; MS (MALDI-TOF) m/z calcd for C₅₂H₉₆N₁₈O₂₅ 1391.44, found 1392.66 [M + H₂O]⁺.

DPA52: IR (neat, cm⁻¹) 3375 (br, OH), 2979, 2932, 2108, 1727, 1686, 1522, 1457; ¹H NMR (500 MHz, D₂O) δ 8.06 (s, 2 H, triazole), 5.95 (d, J = 3.94 Hz, 2 H, H_{1II}), 5.32 (d, J = 3.15 Hz, 2 H, H_{1III}), 5.17 (d, J = 1.26 Hz, 2 H, H_{1IV}), 4.47 (d, J = 1.26 Hz, 2 H), 4.48–4.42 (m, 2 H, H_{4III}), 4.40–4.36 (t, J = 5.20 Hz, 2 H, H_{2III}), 4.24–4.20 (t, J = 4.41 Hz, 2 H, H_{4IV}), 4.14–4.11 (t, J = 2.99 Hz, 2 H, H_{4I}), 4.03–3.98 (t, J = 9.62 Hz, 2 H, H_{6II}), 3.96–3.92 (m, 2 H, H_{5I}), 3.92–3.80 (m, 8 H, H_{2IV}, H_{4IV}, H_{5IV}, H_{3III}), 3.74–3.72 (m, 2 H, H_{6I}), 3.61–3.55 (t, J = 9.14 Hz, 2 H, H_{3II}), 3.54–3.48 (m, 4 H, H_{3I}, H_{5II}), 3.48–3.40 (m, 4 H), 3.38–3.20 (m, 8 H), 2.42–2.35 (dt, J_1 = 3.47 Hz, J_2 = 4.25 Hz, 2 H, H_{2Ieq}), 1.85–1.75 (q, J = 12.61 Hz, 2 H, H_{2Iax}); MS (MALDI-TOF) m/z calcd for C₅₃H₉₈N₁₈O₂₄ 1389.45, found 1389.66 [M + H₂O]⁺. Anal. Calcd for C₅₃H₁₁₀N₁₈O₂₄Cl₁₂: C, 35.19; H, 6.13; Cl, 23.52; N, 13.94; O, 21.23. Found: C, 34.89; H, 6.21; N, 13.71.

DPA53: IR (neat, cm⁻¹) 3368 (br, OH), 2090, 1642; ¹H NMR (500 MHz, D₂O) δ 8.51 (s, 2 H, triazole), 7.91 (s, 4 H, Ar), 6.02 (d, J = 3.60 Hz, 2 H, H_{1II}), 5.39 (d, J = 3.00 Hz, 2 H, H_{1III}), 5.24 (s, 2 H, H_{1IV}), 4.27 (t, J = 4.70 Hz, 2 H), 4.20–4.05 (m, 6 H, H_{5I}, H_{6II}), 4.00–3.80 (m, 6 H), 3.73 (m, 6 H), 3.65 (m, 12 H), 3.55 (m, 8 H), 3.45–3.20 (m, 10 H), 3.18–3.10 (m, 2 H), 2.43–2.35 (dt, J_1 = 4.15 Hz, J_2 = 4.28 Hz, 2 H, H_{2Ieq}), 1.82–1.72 (q, J = 12.45 Hz, 2 H, H_{2Iax}); MS (MALDI-TOF) m/z calcd for C₅₆H₉₆N₁₈O₂₄ 1423.47, found 1424.41 [M + H₂O]⁺; UV (water) λ_{max} = 275 nm. Anal. Calcd for C₅₆H₁₀₈N₁₈O₂₄Cl₁₂: C, 36.49; H, 5.91; Cl, 23.08; N, 13.68; O, 20.83. Found: C, 36.04; H, 5.79; N, 13.31.

Table 1. Linker Structures and Percent Yields (for two steps) for the Synthesis of Dimeric Neomycins

Neomycin dimer	Linker length	Structure of the linker (-x-, from Scheme 1 and Scheme 2)	% yield
DPA51	7		89.5
DPA52	7		88.2
DPA65	7		83.0
DPA53	8		87.0
DPA54	8		88.5
DPA55	14		82.0
DPA56	14		88.8
DPA58	20		83.5
DPA60	24		82.8

DPA54: $^1\text{H NMR}$ (500 MHz, D_2O) δ 7.86 (s, 2 H, triazole), 5.79 (s, 2 H, H_{III}), 5.30 (s, 2 H, H_{III}), 5.20 (s, 2 H, H_{IV}), 4.47 (d, $J = 1.26$ Hz, 2 H), 4.48–4.42 (m, 2 H, H_{III}), 4.38 (t, $J = 5.20$ Hz, 2 H, H_{IIIV}), 4.46 (s, 8 H), 4.25 (s, 4 H), 4.22 (s, 4 H), 4.12 (m, 4 H), 3.97–3.90 (m, 6 H), 3.75–3.65 (m, 10 H), 3.55–3.45 (m, 6 H), 3.40–3.20 (m, 12 H), 3.40–3.23 (m, 12 H), 3.20–3.05 (m, 8 H), 2.38 (d, $J = 12.14$ Hz, 2 H, H_{2Ieq}), 1.70–1.50 (m, 2 H, H_{2Iax}); MS (MALDI-TOF) m/z calcd for $\text{C}_{54}\text{H}_{100}\text{N}_{18}\text{O}_{24}$ $[\text{M} + \text{H}_2\text{O}]^+$ 1405.48, found 1404.64; UV (water) $\lambda_{\text{max}} = 225$ nm.

DPA55: $^1\text{H NMR}$ (500 MHz, D_2O) δ 7.82 (s, 2 H, triazole), 5.95 (s, 2 H, H_{III}), 5.33 (s, 2 H, H_{III}), 5.22 (s, 2 H, H_{IV}), 4.55–4.43 (br, 4 H, H_{III}), 4.24 (m, 2 H), 4.13 (s, 2 H), 3.99 (m, 2 H), 3.95–3.80 (m, 8 H), 3.78–3.70 (4 H), 3.66–3.58 (m, 4 H), 3.56 (m, 2 H), 3.54 (s, 2 H), 3.51 (s, 2 H), 3.45–3.35 (m, 6 H), 3.34–3.30 (s, 2 H), 3.30–3.19 (m, 6 H), 2.40–2.31 (m, 6 H), 2.26 (m, 2 H, H_{2Ieq}), 1.81–1.72 (m, 2 H, H_{2Iax}); MS (MALDI-TOF) m/z calcd for $\text{C}_{58}\text{H}_{106}\text{N}_{18}\text{O}_{24}$ $[\text{M} + \text{H}_2\text{O}]^+$ 1456.77, found 1457.90; UV (water) $\lambda_{\text{max}} = 227$ nm.

DPA56: $^1\text{H NMR}$ (500 MHz, D_2O) δ 7.80 (s, 2 H, triazole), 6.00 (d, $J = 3.63$ Hz, 2 H, H_{III}), 5.36 (d, $J = 2.84$ Hz, 2 H,

H_{III}), 5.21 (s, 2 H, H_{IV}), 4.53–4.47 (m, 4 H, H_{III}), 4.45 (t, $J = 5.05$ Hz, 2 H), 4.23 (t, $J = 5.36$ Hz, 4 H), 4.17–4.11 (m, 6 H), 3.97 (t, $J = 9.77$ Hz, 4 H, H_{5IV} , H_{6II}), 3.93–3.83 (m, 8 H, H_{2IV} , H_{4IV} , H_{5IV} , H_{3III}), 3.75–3.70 (m, 6 H), 3.69–3.59 (m, 10 H), 3.55–3.59 (m, 2 H), 3.54 (s, 4 H), 3.50–3.53 (m, 4 H), 3.43–3.34 (m, 8 H), 3.34–3.24 (m, 8 H), 3.22–3.15 (m, 8 H), 2.64–2.58 (m, 4 H), 2.40–2.33 (m, 2 H, H_{2Ieq}), 1.96 (m, 6 H, H_{2Iax} and protons from linker), 1.55 (m, 4 H, protons from linker); MS (MALDI-TOF) m/z calcd for $\text{C}_{56}\text{H}_{104}\text{N}_{18}\text{O}_{24}$ $[\text{M} + \text{Na}]^+$ 1435.53, found 1434.83; UV (water) $\lambda_{\text{max}} = 227$ nm. Anal. Calcd for $\text{C}_{56}\text{H}_{116}\text{N}_{18}\text{O}_{24}\text{Cl}_{12}$: C, 36.34; H, 6.32; Cl, 22.98; N, 13.62; O, 20.74. Found: C, 36.24; H, 6.11; N, 13.41.

DPA58: $^1\text{H NMR}$ (500 MHz, D_2O) δ 8.06 (s, 2 H, triazole), 5.97 (d, $J = 3.47$ Hz, 2 H, H_{III}), 5.33 (d, $J = 3.00$ Hz, 2 H, H_{III}), 5.22 (s, 2 H, H_{IV}), 4.80–4.74 (m, 2 H), 4.51–4.43 (m, 4 H, H_{III}), 4.24 (t, $J = 4.42$ Hz, 2 H), 4.13 (t, $J = 2.37$ Hz, 2 H), 3.97 (t, $J = 9.61$ Hz, 2 H, H_{6II}), 3.93 (t, $J = 10.40$ Hz, 2 H), 3.90–3.78 (m, 6 H), 3.76–3.70 (m, 4 H), 3.69–3.58 (m, 8 H), 3.57–3.53 (m, 6 H), 3.52–3.47 (m, 6 H), 3.44 (t, $J = 9.14$ Hz, 4 H), 3.41–3.34 (m, 4 H), 3.32 (t, $J = 6.14$ Hz,

2 H), 3.30–3.16 (m, 6 H), 2.41–2.33 (dd, $J_1 = 3.94$ Hz, $J_2 = 3.62$ Hz, 2 H), 1.84–1.72 (q, $J = 13.24$ Hz, 2 H, $H_{2\text{max}}$), 1.53–1.43 (m, 4 H, linker protons), 1.25–1.14 (m, 8 H, linker protons), 1.13–1.04 (t, $J = 6.62$ Hz, 4 H, linker protons); MS (MALDI-TOF) m/z calcd for $C_{60}H_{112}N_{18}O_{26}$ [$M + 2H_2O$] $^+$ 1537.64, found 1538.11; UV (water) $\lambda_{\text{max}} = 229$ nm.

DPA60: ^1H NMR (500 MHz, D_2O) δ 8.05 (s, 2 H, triazole), 5.97 (d, $J = 3.78$ Hz, 2 H, H_{III}), 5.34 (d, $J = 3.31$ Hz, 2 H, H_{III}), 5.22 (s, 2 H, H_{IV}), 4.55 (s, 4 H), 4.50–4.46 (m, 2 H, H_{III}), 4.43 (t, $J = 4.57$ Hz, 2 H), 4.23 (t, $J = 4.42$ Hz, 2 H), 4.19–4.15 (m, 2 H), 3.94 (t, $J = 2.53$ Hz, 2 H), (N 4.05 (t, $J = 9.93$ Hz, 2 H), 3.96–3.90 (t, $J = 10.25$ Hz, 2 H), 3.90–3.79 (m, 8 H), 3.76–3.69 (m, 6 H), 3.70–3.58 (m, 12 H), 3.55–3.42 (m, 12 H), 3.42–3.38 (m, 2 H), 3.38–3.35 (m, 2 H), 3.34–3.30 (m, 4 H), 3.30–3.22 (m, 6 H), 2.38 (dd, $J_1 = 4.10$ Hz, $J_2 = 4.73$ Hz, 2 H), 1.85–1.75 (q, $J = 11.98$ Hz, 2 H, $H_{2\text{max}}$), 1.54–1.41 (m, 4 H, linker protons), 1.24–1.10 (m, 18 H, linker protons); MS (MALDI-TOF) m/z calcd for $C_{64}H_{120}N_{18}O_{26}$ [$M + H_2O$] $^+$, found 1576.11; UV (water) $\lambda_{\text{max}} = 228$ nm.

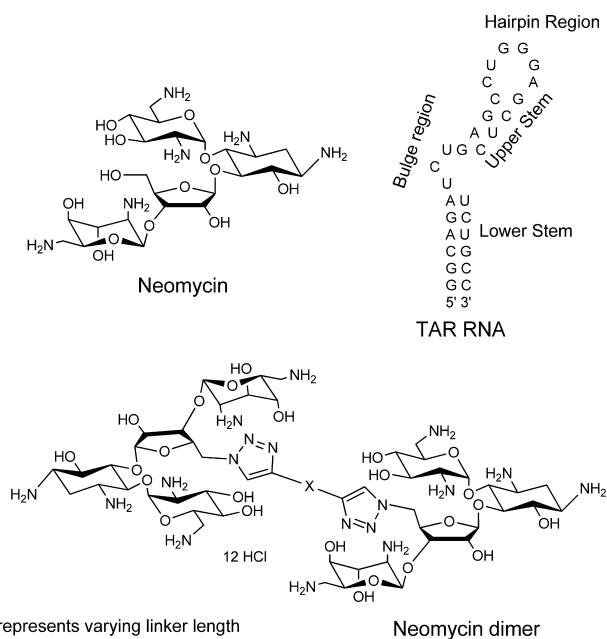
DPA65: IR (neat, cm^{-1}) 3434 (br, OH), 2086 (weak), 1637; ^1H NMR (500 MHz, D_2O) δ 8.52 (s, 2 H, triazole), 8.24 (s, 1 H, Ar), 7.80 (d, $J = 7.72$ Hz, 2 H, Ar), 7.58 (t, $J = 7.88$ Hz, 1 H, Ar), 5.94 (d, $J = 3.62$ Hz, 2 H, H_{III}), 5.38 (d, $J = 3.00$ Hz, 2 H, H_{III}), 5.25 (d, $J = 1.10$ Hz, 2 H, H_{IV}), 4.90–4.83 (m, 2 H, H_{III}), 4.81–4.76 (m, 2 H), 4.64–4.56 (m, 6 H), 4.24 (t, $J = 4.73$ Hz, 2 H), 4.16 (t, $J = 4.10$ Hz, 2 H), 4.13 (t, $J = 2.99$ Hz, 2 H), 4.05 (t, $J = 9.77$ Hz, 4 H, $H_{5\text{B}}$, $H_{6\text{II}}$), 3.95–3.85 (m, 6 H), 3.85–3.79 (m, 2 H), 3.74–3.71 (m, 2 H), 3.67–3.59 (m, 4 H), 3.58–3.49 (m, 8 H), 3.49–3.38 (m, 4 H), 3.47–3.34 (m, 2 H), 3.47–3.31 (m, 4 H), 3.31–3.29 (m, 4 H), 3.29–3.22 (m, 6 H), 3.07–3.01 (m, 2 H), 2.37 (dd, $J_1 = 4.10$ Hz, $J_2 = 4.25$ Hz, 2 H, $H_{2\text{leq}}$), 1.82–1.72 (q, 2 H, $H_{2\text{max}}$); MS (MALDI-TOF) m/z calcd for $C_{56}H_{96}N_{18}O_{24}$ ($M + Na^+$) 1423.47, found 1424.41 [$M + H_2O$] $^+$; UV (water) $\lambda_{\text{max}} = 236$ nm. Anal. Calcd for $C_{56}H_{108}N_{18}O_{24}Cl_{12}$: C, 36.49; H, 5.91; Cl, 23.08; N, 13.68; O, 20.83. Found: C, 36.22; H, 5.81; N, 13.48.

RESULTS AND DISCUSSION

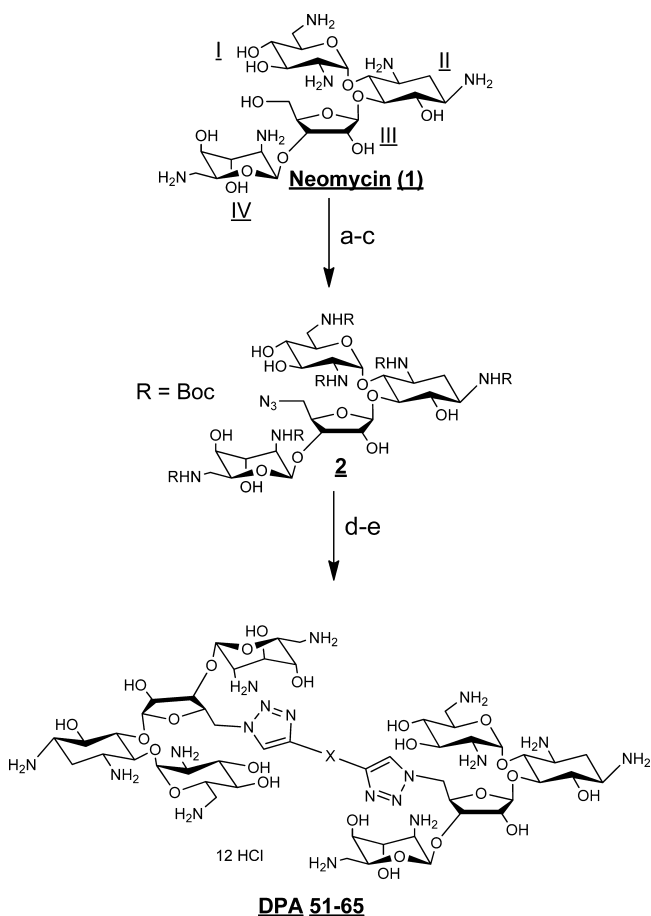
Design and Synthesis of Triazole-Linked Neomycin Dimers. Previous ESI-MS data have shown that neomycin has at least two binding sites on HIV TAR RNA.⁵² One binding site has been reported to be below the trinucleotide bulge region (see Scheme 1 for structures), and the second binding site lies in the upper stem or hairpin region. To take advantage of these multiple sites and to improve ligand affinity and selectivity, we synthesized a series of neomycin dimers. The neomycin dimers were synthesized using a high-yielding, inert, and robust synthetic “click chemistry” approach as shown in Scheme 2.^{54–56} The length and functionality of the linker that tethers the two neomycin units have been varied to investigate the optimal binding interaction between neomycin dimers and HIV TAR RNA. Azide **2** was synthesized in three steps from commercially available neomycin **1**⁵⁷ and then reacted with terminal dialkynes in a 2:1 ratio to yield the triazole-linked dimers (Scheme 2). Deprotection of *tert*-butoxycarbonyl (Boc) groups using 4 N HCl in dioxane yielded the dimer hydrochloride salts^{58–61} DPA52–DPA65 in excellent yields.

Neomycin Dimers Significantly Enhance the Thermal Stability of HIV TAR RNA. UV thermal denaturation studies were conducted with the dimers and HIV 1 TAR RNA (Figure 1 and Table 2; see section S3 of the Supporting Information for UV denaturation plots). Neomycin dimers

Scheme 1. Structures of Small Molecule Ligands (neomycin and neomycin dimer) and TAR RNA Used in This Study



Scheme 2. ^a



^aReagents and conditions: (a) (Boc)₂O, DMF, H₂O, Et₃N, 60 °C, 5 h, 60%; (b) TPS-Cl, pyridine, room temperature, 40 h, 50%; (c) NaN₃, DMF/H₂O (10:1), 12 h, 90 °C, 90%; (d) toluene, CuI, DIPEA, 90 °C; (e) 4 N HCl in dioxane, room temperature, 5 min. Yield for steps d and e of 82–90%.

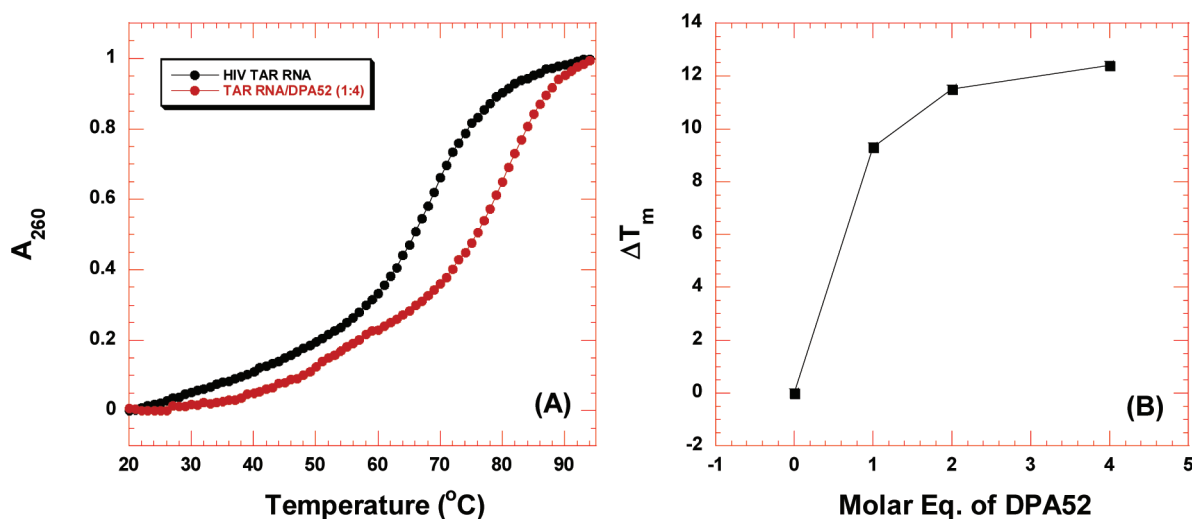


Figure 1. Concentration dependent UV thermal denaturation profile of HIV TAR RNA with neomycin dimer DPA52. UV thermal denaturation data of HIV TAR RNA with no DPA52, and 4 μM (4 mol equiv) of DPA52 (A). Plot showing the change in thermal stabilization (ΔT_m) as a function of molar equivalents of DPA52 (B). Buffer conditions: 100 mM KCl, 10 mM SC, 0.5 mM EDTA, pH 6.8. [HIV TAR RNA] = 1 μM /strand. The heating rate was 0.3 $^{\circ}\text{C}$.

Table 2. UV Thermal Denaturation Data of HIV TAR RNA in the Presence of Increasing Concentrations of Neomycin Dimer DPA52^a

DPA52:TAR RNA ratio	T_m ($^{\circ}\text{C}$)	ΔT_m ($^{\circ}\text{C}$)
TAR RNA	68.9	–
1	78.2	9.3
2	80.4	11.5
4	81.3	12.4

^aBuffer conditions: 100 mM KCl, 10 mM SC, 0.5 mM EDTA, pH 6.8. The HIV TAR RNA concentration was 1 μM /strand. The heating rate was 0.3 $^{\circ}\text{C}$.

significantly enhance the thermal stability of HIV TAR RNA [$\Delta T_m = 3.3\text{--}10.2$ $^{\circ}\text{C}$ (Table 2)]. The level of thermal stabilization of HIV TAR RNA by neomycin dimers decreases with increasing linker length between the two neomycin units. The UV thermal denaturation data indicate that the probable binding sites of two neomycin units are in the proximity of each other. Additionally, neomycin displayed no thermal stabilization of TAR RNA, as opposed to the neomycin dimers. There was very little thermal stabilization observed ($\Delta T_m = 0.5$ $^{\circ}\text{C}$) of HIV TAR RNA even when the concentration of neomycin was increased above a 1:1 ratio.

The UV denaturation data suggest that the thermal stabilization of HIV TAR RNA by neomycin dimers is a result of specific interaction as opposed to a nonspecific electrostatic cation (neomycin dimers)–anion (HIV TAR RNA) interaction. To further validate our assumption, a concentration-dependent thermal denaturation study was performed in which the concentration of the dimer was varied at a fixed RNA concentration. UV thermal denaturation of HIV TAR RNA was monitored at 2 molar equiv of neomycin dimers, and the results are summarized in Table 3. Additionally, a concentration-dependent UV thermal denaturation study was conducted with HIV TAR RNA and DPA52 [up to 4 molar equiv of DPA52 (Figure 1)], and the results are also summarized in Table 2.

There are few important points to be noted. (1) There was only 2–3 $^{\circ}\text{C}$ additional thermal stabilization observed in going from 1 to 2 molar equiv of neomycin dimers. This is in contrast to the UV thermal stabilization of HIV TAR RNA of ~ 11 $^{\circ}\text{C}$,

when going from a 0:1 to a 1:1 ratio (neomycin dimer:HIV TAR RNA). (2) The UV thermal denaturation of HIV TAR RNA with an increase in the amount of all the neomycin dimers from 1 to 2 molar equiv shows the same change in T_m (2–3 $^{\circ}\text{C}$). (3) There was a thermal stabilization of 12.4 $^{\circ}\text{C}$ observed for HIV TAR RNA in the presence of 4 molar equiv of DPA52 in comparison to a value of 9.3 $^{\circ}\text{C}$ at 1 molar equiv. The thermal denaturation data suggest that in all likelihood (1) a specific binding interaction takes place between neomycin dimers and HIV TAR RNA at a binding stoichiometry of 1:1 (neomycin dimer:HIV TAR RNA). The concentration-dependent study suggests that binding of the neomycin dimer to HIV TAR RNA is not simply a result of charge interactions but involves potential and shape complementarity to the RNA target. (2) A higher molar ratio of the neomycin dimer does not enhance the UV thermal stability significantly. It is indicative of a 1:1 binding ratio between neomycin dimer and HIV TAR RNA. (3) Addition of a large excess of neomycin to TAR does not have any effect on the thermal stability of HIV TAR RNA, suggesting that the sum of the monomer parts clearly leads to a much improved ligand with enhanced RNA affinity.

CD Spectroscopy Studies for Characterizing the Binding between the Neomycin Dimer and HIV TAR RNA. CD spectroscopy is a powerful tool for monitoring and characterizing the binding interaction between macromolecules (nucleic acids and proteins) and ligands.^{32,33} CD spectroscopy can provide useful insight into the change in the conformation of the macromolecule during the binding reaction.³² CD spectroscopy was used to investigate the binding interaction between the neomycin dimer and HIV TAR RNA. The CD spectrum of HIV TAR RNA consists of a strong positive peak at 265 nm and an equally strong peak with a negative magnitude at 211 nm. Additionally, there is a negative peak observed at ~ 240 nm. This CD spectrum is indicative of an A-form conformation. Earlier CD studies of the Tat–HIV TAR RNA complex revealed a substantial change in the structure of HIV TAR RNA induced by Tat protein. During the Tat–HIV TAR RNA binding interaction, there is a slight red shift observed at 265 nm. Additionally, the CD intensity of HIV TAR RNA at 265 nm decreases by 15%.⁶² The CD peak at 265 nm is a signature peak for the

Table 3. Representative UV Thermal Denaturation Data of Ligand–HIV TAR RNA Complexes at r_{dr} Values of 1 and 2^a

	T_m (°C)	ΔT_m (°C) (at $r_{dr} = 1$)	$\Delta\Delta T_m$ (°C) ($r_{dr} = 2 - r_{dr} = 1$)
HIV 1 TAR RNA	68.9	NA ^b	NA ^b
DPAS1	79.1	10.2	2.8
DPAS2	78.2	9.3	2.5
DPA65	78.2	9.3	2.1
DPAS3	78.5	9.6	2.9
DPAS4	77.1	8.2	2.2
DPAS5	76.4	7.6	2.8
DPAS6	74.9	6.1	3.2
DPAS8	74.3	5.4	2.9
DPA60	72.1	3.3	3.0
neomycin	69.1	0.2	0.4

^a r_{dr} is the ratio of neomycin dimer to HIV TAR RNA. Buffer conditions: 100 mM KCl, 10 mM SC, 0.5 mM EDTA, pH 6.8. The HIV TAR RNA concentration was 1 μ M/strand. The neomycin dimer concentrations were 1 and 2 μ M. The neomycin concentrations were 1 and 2 μ M. ^bNot applicable.

trinucleotide bulge region (UCU) and has been attributed to the arrangement of base stacking in the bulge region.²² During the Tat–HIV TAR RNA interaction, the Tat protein binds at its primary binding site, which is the trinucleotide region, and modifies the arrangement of base stacking in the bulge region. The binding interaction was monitored by a decrease in the CD intensity at 265 nm. There is a marginal red shift observed at 265 nm, indicative of the small distortion of the A-form structure.

A CD titration was performed with the neomycin dimer and HIV TAR RNA by continuous addition of the dimer to an HIV TAR RNA solution (Figure 2A). The overall shapes of the CD spectra in the absence and presence of the dimer are similar, suggesting that the overall conformation of HIV TAR RNA is conserved. There are some changes observed in the spectrum of HIV TAR RNA upon addition of the dimer. The addition of the neomycin dimer causes a gradual decrease in the magnitudes of the peaks at 210 and 240 nm. Contrary to Tat protein binding, there was no change in the CD intensity of the HIV TAR RNA–dimer complex at 265 nm; however, a red shift was observed. This observation suggests that the dimer does not interact with the trinucleotide bulge region (Figure 2A). However, the interaction of the neomycin dimer causes a slight distortion of the A-form conformation of HIV TAR RNA and pushes it toward B-form. All these observations collectively provide insight into the probable binding site of the neomycin dimer on HIV TAR RNA. The primary binding site of neomycin is just below the trinucleotide bulge region (see Scheme 1); hence, one unit of neomycin likely binds to the lower stem region of HIV TAR RNA, and the second neomycin unit binds to the upper stem or the hairpin region. Further structural studies aim to evaluate the effect of dimer binding on RNA conformation and will be reported in due course.

CD spectroscopy is useful in identifying global changes in the macromolecule structure, but it also can provide valuable information about the binding stoichiometry of ligands involved in the study.³³ The change in CD intensity was plotted as a function of neomycin dimer:HIV TAR RNA molar ratio, and the plot results in an inflection point (Figure 2B) suggesting that the binding stoichiometry is 1:1 (neomycin dimer:HIV TAR RNA). To verify the results of CD spectroscopy, an FID (fluorescent intercalator displacement) titration was also per-

formed⁶³ (ethidium bromide as an intercalator) (Figure 2C). The change in fluorescence was plotted as a function of the number of molar equivalents of the neomycin dimer, and the inflection point also allows us to estimate the neomycin dimer:HIV TAR RNA binding stoichiometry. Both CD and FID titration data reveal a 1:1 neomycin dimer:HIV TAR RNA binding stoichiometry.

Ethidium Bromide Displacement and FRET Competition Binding Assay for Characterizing the Binding of Neomycin Dimers to HIV TAR RNA. To further investigate the binding between HIV TAR RNA and neomycin dimers, ethidium bromide displacements⁶³ were performed, and the results are summarized in Table 4 (see section S4 of the Supporting Information for FID assay plots). The affinities of neomycin dimers are directly proportional to the amount of ethidium bromide displaced from HIV TAR RNA and reflected in the IC₅₀ (the concentration of ligand required to displace 50% ethidium bromide from HIV TAR RNA) values. Ethidium bromide displacement experiments indicate that in general, neomycin dimers with shorter linker lengths have a higher affinity for HIV TAR RNA than neomycin dimers with a longer linker. The IC₅₀ values for neomycin dimers fall within a range of 36–99 nM. In comparison to neomycin dimers, neomycin has a very low affinity for HIV TAR RNA. The IC₅₀ value of neomycin toward HIV TAR RNA is 417 ± 115 nM. The trend of linker length versus IC₅₀ values observed here is the same as that observed for linker length versus δT_m values from UV thermal denaturation experiments. These results also indicate that the two neomycin binding sites on HIV TAR RNA are very close to each other. Hence, the neomycin dimers with shorter linkers bind tightly, as reflected in the lower IC₅₀ and stronger thermal stabilization toward HIV TAR RNA.

The CD titration and UV denaturation data show that the dimers bind with a stoichiometry of 1:1 with TAR RNA. We therefore performed ethidium bromide displacement titrations between HIV TAR RNA and the neomycin dimer to determine the association constant using Scatchard analysis⁶³ (Figure 3A–D). The plot between the change in fluorescence and the number of molar equivalents of neomycin dimer(s) to TAR RNA was used (as described above) to determine the binding stoichiometry of neomycin dimer toward HIV TAR RNA (Figure 3B). The data from ethidium bromide (EtBr) displacement titrations were analyzed and transformed using Scatchard analysis (Figure 3C). The slope of the plot allows us to determine the association constant of neomycin dimer(s) with HIV TAR RNA (Figure 3D).

FID titrations were performed with all the neomycin dimers and the neomycin monomer (see section S6 of the Supporting Information for FID titrations) with TAR RNA, and the results are summarized in Table 5. The binding constant for binding of neomycin to TAR RNA could not be determined using this analysis, because of the weak affinity of neomycin for HIV TAR RNA (as indicated by the small displacement of EtBr). This is consistent with the earlier observations (UV melt and FID assay) that show a weak affinity of neomycin for HIV TAR RNA.

A comparison was then made between the linker lengths of neomycin dimers and the binding constants derived from Scatchard analysis (Figure 4). The binding constant decreases with an increase in the length of the linker. Neomycin dimer DPA56 (linker length of 10) was an exception, as it showed a higher affinity than DPA54 with a linker length of 8, but still much lower affinity than dimers with linker lengths of 7 or 8. The trend in binding constant versus K_a was compared with the data from the UV thermal denaturation experiment (Figure 4). The trends are similar

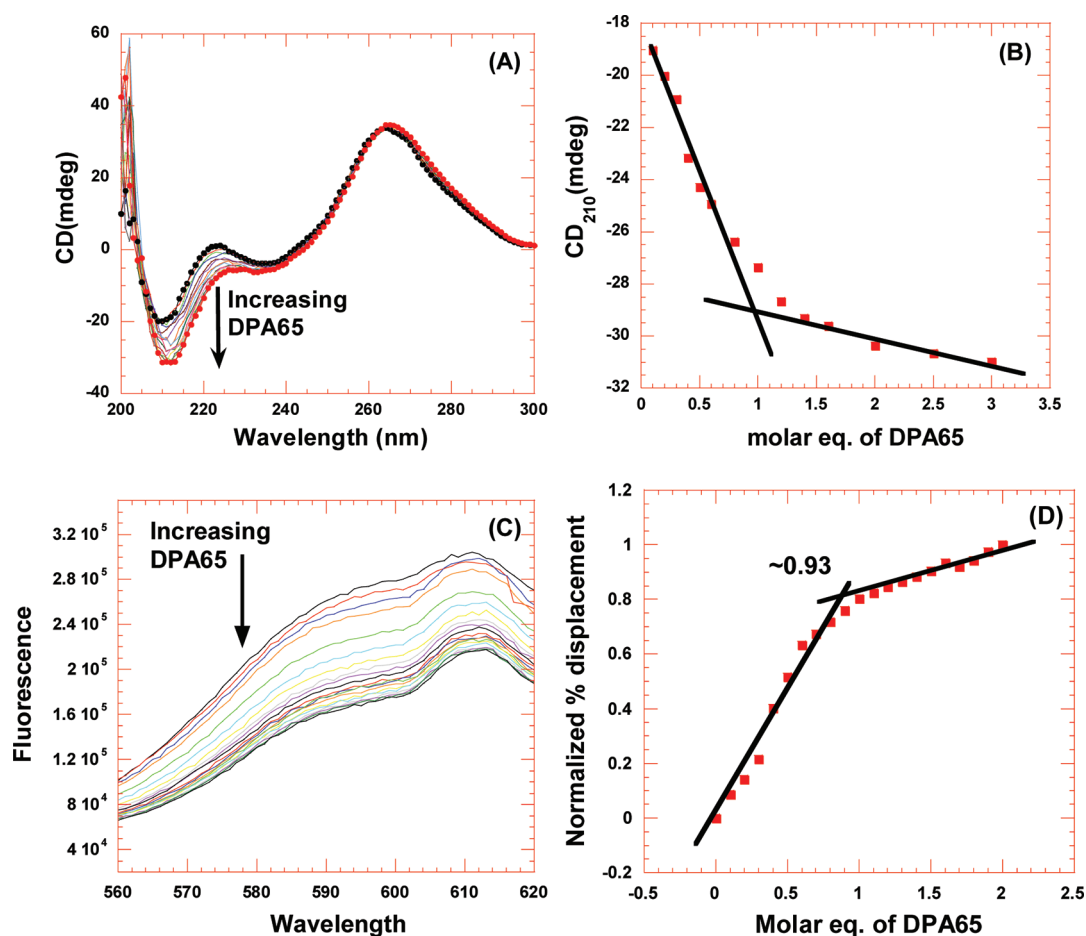


Figure 2. Comparison of CD titration and FID titration for determining the binding stoichiometry between HIV TAR RNA and DPA65. (A) CD titration of HIV TAR RNA with increasing concentrations of the neomycin dimer. This figure represents the molar ellipticity for CD titration of HIV TAR RNA with the neomycin dimer. The continuous changes in the CD spectra correspond to the incremental amount of neomycin dimer ranging from an r_{dr} of 0 to an r_{dr} of 3. (B) Plot of normalized molar ellipticity vs r_{dr} for CD titration of HIV TAR RNA with the neomycin dimer. The solid lines reflect the linear least-squares fit of each apparent linear domain of the experimental data (red square) before and after the apparent inflection point. (C) Raw fluorescence emission spectra in the presence of increasing concentrations of DPA65. (D) The plot of the normalized fluorescence intensity (at 605 nm) of the HIV TAR RNA–ethidium bromide complex as a function of DPA65 concentration results in a saturating binding plot. For CD, the molar ellipticity is per molecule of HIV TAR RNA, and r_{dr} is the drug:HIV TAR RNA ratio. The HIV TAR RNA concentration was 4 μM /strand. For FID titration, the HIV TAR RNA concentration was 100 nM/strand.

Table 4. Representative Data from an Ethidium Bromide Displacement Assay^a

ligand	linker length	IC ₅₀ (nM)
DPAS1	7	56
DPAS2	7	52
DPA65	7	36
DPAS3	8	67
DPAS4	8	81
DPAS5	10	99
DPAS6	10	97
DPAS8	16	67
DPA60	20	74
neomycin	NA ^b	417

^aBuffer conditions: 100 mM KCl, 10 mM SC, 0.5 mM EDTA, pH 6.8. The HIV TAR RNA concentration was 50 nM/strand. ^bNot applicable.

if not identical. The binding constant decreases with an increase in linker length; similarly, the UV thermal stabilization of HIV TAR decreases with an increase in neomycin dimer linker length.

Salt-Dependent Studies of the Neomycin Dimer with TAR RNA. We then studied the effect of salt on the binding between the neomycin dimer and HIV TAR RNA. FID titrations were conducted at three different salt concentrations (Figure 5), and the data was analyzed and fit using Scatchard analysis to determine the binding constants. The binding constants at three different salt concentrations are summarized in Table 6.

The binding affinity of neomycin dimer DPA52 for HIV TAR RNA continuously decreases with an increase in the KCl concentration from 50 to 150 mM. The salt-dependent binding parameters were used to calculate the number of ion pairs formed during the association of the neomycin dimer and HIV TAR RNA, as described by Record.⁶⁴ In the case of HIV TAR RNA–neomycin dimer interaction, there are two or three ion pairs between the ligand and RNA. The free energy of the electrolytic contribution was then calculated using eq 1.^{64,65}

$$\Delta G_{pe} = -Z\phi RT \ln[\text{KCl}] \quad (1)$$

where Z denotes the charge on the ligand and ϕ is the number of the counterions associated with each phosphate group on nucleic acid that normally varies for nucleic acids. The value of

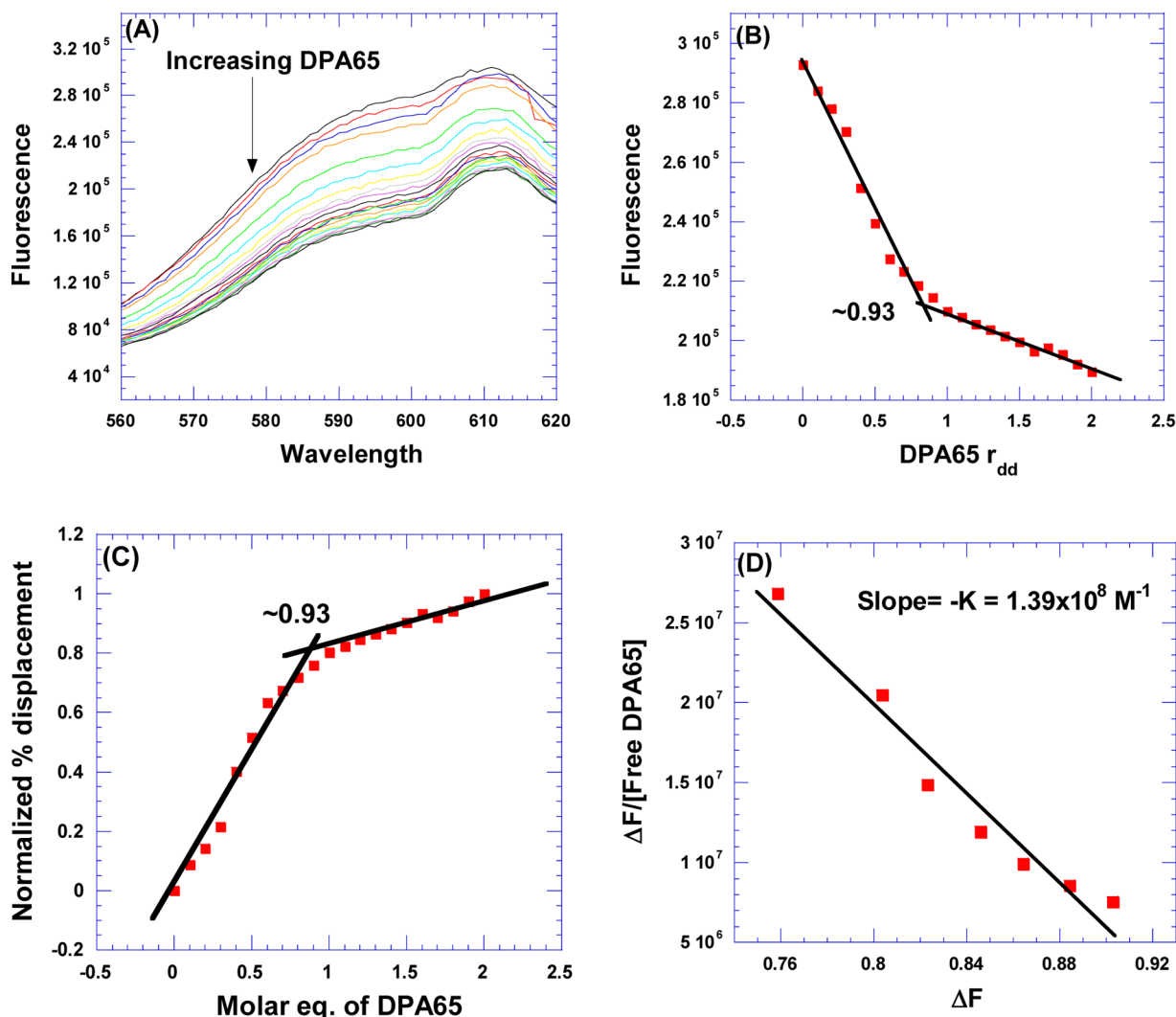


Figure 3. FID titration of DPA65 with HIV TAR RNA. (A) Raw fluorescence emission spectra in the presence of increasing concentrations of DPA65. (B) The decrease in fluorescence intensity (at 605 nm) of the HIV TAR RNA–EtBr complex with an increasing concentration of DPA65 results in a saturating binding plot. (C) The plot between normalized fluorescence intensity (at 605 nm) of the HIV TAR RNA–EtBr complex as a function of DPA65 concentration results in a saturating binding plot. (D) Scatchard plot analysis of DPA65 with HIV TAR RNA. Buffer conditions: 100 mM KCl, 10 mM SC, 0.5 mM EDTA, pH 6.8. The HIV TAR RNA concentration was 200 nM/strand. The EtBr concentration was 5 μ M.

Table 5. Representative Binding Constants Derived from Scatchard Analysis of the FID Assay (ethidium bromide as an intercalator) between the Neomycin Dimer and HIV TAR RNA^a

	linker length	K (M^{-1})
DPAS1	7	1.17×10^8
DPAS2	7	7.08×10^7
DPA65	7	1.39×10^8
DPAS3	8	1.46×10^8
DPAS4	8	2.61×10^7
DPAS5	10	1.06×10^7
DPAS6	10	6.60×10^7
DPAS8	16	7.58×10^6
DPA60	20	2.53×10^7
neomycin	NA ^b	–

^aBuffer conditions: 100 mM KCl, 10 mM SC, 0.5 mM EDTA, pH 6.8. The HIV TAR RNA concentration was 200 nM/strand. The EtBr concentration was 5 μ M. ^bNot applicable.

ϕ for the A-form RNA duplex [poly(rA)·poly(rU)] is 0.89, while that for single-stranded RNA [poly(rA)] is 0.78. HIV

TAR RNA contains hairpin, bulge, and duplex regions; therefore, it is likely that the value of ϕ falls within the range of these two values, and hence, the average of these two values was used in the analysis. The free energy of the electrolytic contribution was calculated by inserting the experimental values into eq 1. The electrolytic contribution to the free energy (ΔG_{pe}) obtained is -3.45 kcal/mol at 100 mM KCl, and the total free energy of interaction (ΔG_{obs}) is -10.69 kcal/mol. The free energy contribution of nonelectrolytic energy was calculated using eq 2 as -7.24 kcal/mol (Figure 6).

$$\Delta G_{obs} = -RT \ln K = \Delta G_{pe} + \Delta G_{non-pe} \quad (2)$$

Figure 6 shows that the major contribution to the binding event between the neomycin dimer and HIV TAR RNA is nonelectrolytic. This observation provides further insight into the mode of binding of the neomycin dimer to HIV TAR RNA. Though the dimer is a highly positively charged ligand (12 aliphatic amines, 10 of which are expected to be protonated at physiological pH), the free energy of the electrolytic contribution does not play a major part in the binding to RNA. The observation suggests that the shape complementarity of the

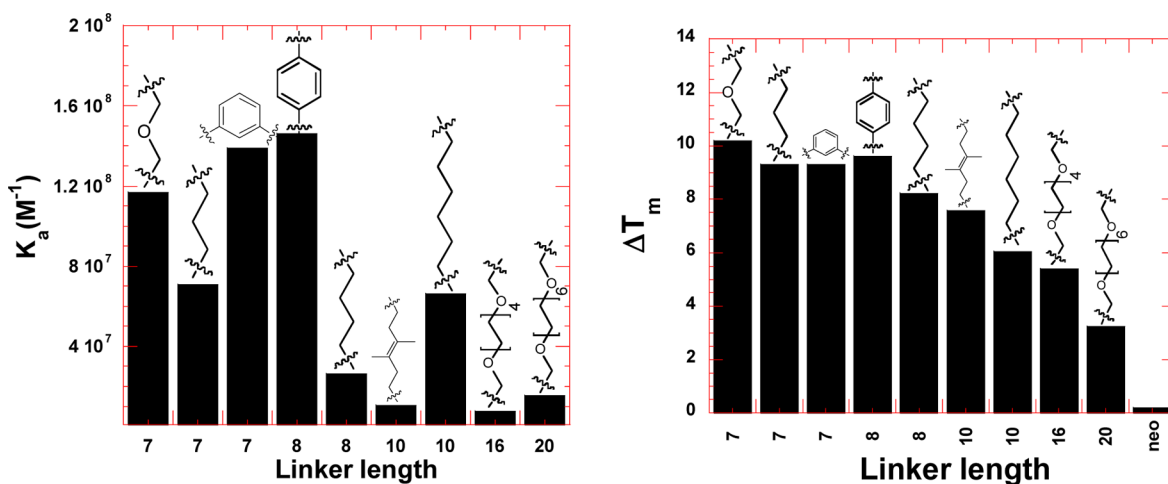


Figure 4. Bar graph showing the comparison of binding constants derived from Scatchard analysis of the FID titrations (ethidium bromide as an intercalator) (left) and UV thermal denaturation profile of neomycin dimers with HIV TAR RNA (right). Buffer conditions: 100 mM KCl, 10 mM SC, 0.5 mM EDTA, pH 6.8. For FID titration, the HIV TAR RNA concentration was 200 nM/strand. For the UV thermal denaturation experiment, the HIV TAR RNA concentration was 1 μ M/strand. The neomycin dimer concentration was 1 μ M. The neomycin concentration was 1 μ M.

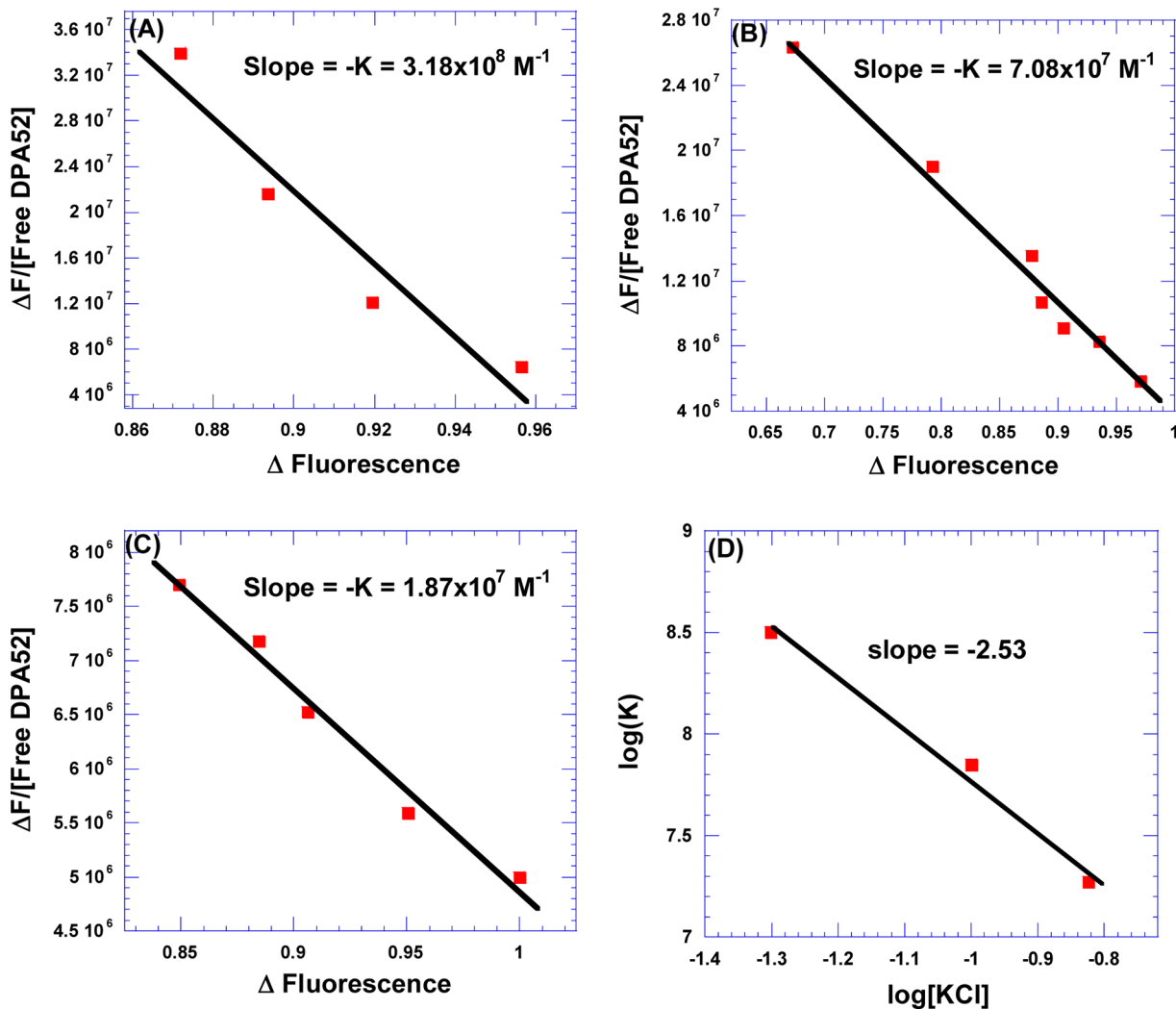


Figure 5. Salt-dependent studies between neomycin dimer DPA52 and HIV TAR RNA. The binding constants were determined from the FID titration using Scatchard plot analysis at (A) 50, (B) 100, and (C) 150 mM KCl. (D) Plot of $\log(K)$ as a function of $\log[KCl]$ fit with linear regression. The solid line reflects the linear fit that results in a slope that reflects the number of ion pairs forming between DPA52 and HIV TAR RNA. Buffer conditions: 10 mM SC, 0.5 mM EDTA, pH 6.8. The HIV TAR RNA concentration was 200 nM/strand. The EtBr concentration was 5 μ M.

Table 6. Representative Binding Constants Derived from Scatchard Analysis Showing the Salt Dependence of Binding between DPAS2 and HIV TAR RNA^a

[KCl] (mM)	<i>K</i> (M ⁻¹)
50	3.18 × 10 ⁸
100	7.08 × 10 ⁷
150	1.87 × 10 ⁷

^aBuffer conditions: 10 mM SC, 0.5 mM EDTA, pH 6.8. The HIV TAR RNA concentration was 200 nM/strand. The EtBr concentration was 5 μM.

neomycin dimer to the TAR RNA conformation is largely responsible for the high binding affinity of this highly positively charged pharmacophore toward HIV TAR RNA.

Fluorescence Resonance Energy Transfer-Mediated Competition Binding Assay. A FRET-mediated fluoremetric competition binding assay was performed to characterize the binding interaction of neomycin dimers with HIV TAR RNA. The assay developed by Hamashaki and co-workers⁵³ is very useful in defining the binding interaction of ligands with HIV TAR RNA. This particular assay is different from the ethidium bromide displacement assay. The assay gives direct competition

among an analogue of Tat protein, a fluorescently labeled Tat peptide, and the ligands used in the study. In this assay, the Tat_{49–57} peptide was functionalized using fluorescein dye at its N-terminus and tetramethyl rhodamine dye at the C-terminus to collectively form a FRET system.⁵³

The fluorescein-labeled Tat_{49–57} peptide was first titrated against HIV TAR RNA to determine its affinity (Figure 7). The fluorescence increases with an increase in the concentration of HIV TAR RNA in a fluorescein-labeled Tat_{49–57} peptide solution and reaches a constant value at a saturating concentration of HIV TAR RNA. Dimers were then titrated against the fluorescein-labeled Tat_{49–57} peptide with an HIV TAR RNA solution (Figure 8; see section S5 of the Supporting Information for FRET assays). The binding affinity of ligands is directly related to the decrease in the fluorescence. The FRET assay was performed with neomycin dimers and neomycin, and the results are summarized in Table 7. The IC₅₀ value of neomycin is almost 1 order of magnitude higher than that of the neomycin dimers, suggesting much higher affinities for the dimers toward HIV TAR RNA than the monomer neomycin. The IC₅₀ value of fluorescein-labeled Tat_{49–57} peptide is 86 ± 9 nM. Neomycin dimers show IC₅₀ values in the range of 47–80 nM. In general, neomycin dimers exhibit higher binding affinities for HIV TAR RNA than neomycin or the Tat_{49–57} peptide does. The FRET results for dimer–TAR RNA binding are consistent with the data obtained from the aforementioned techniques such as UV thermal denaturation and ethidium bromide displacement.

The results of the FRET-mediated assay showed that neomycin dimers exhibit nanomolar affinity toward HIV TAR RNA. A comparison of binding affinity can be made with the earlier reported neamine dimers (Figure 9). Previously reported neamine dimers showed IC₅₀ values in the range of 150–400 nM (pH 7.4 in 50 mM Tris-HCl and 20 mM KCl) using a FRET-mediated competition binding assay and have much lower affinities compared to those of neomycin dimers reported here (47–128 nM at pH 7.4 in 50 mM Tris-HCl and 20 mM KCl). The results clearly show a 3–4-fold preference of neomycin dimers versus neamine dimers for HIV TAR RNA.⁵¹ These observations acknowledge the contribution of rings 3 and 4 in neomycin–HIV TAR RNA binding.

The affinity of neomycin dimers for HIV TAR RNA was compared using FRET and ethidium bromide FID assays

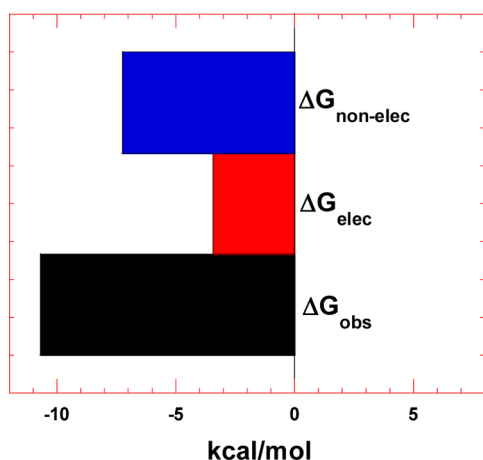


Figure 6. Bar graph showing the dissection of the free energy into its components, including electrolytic and nonelectrolytic contributions.

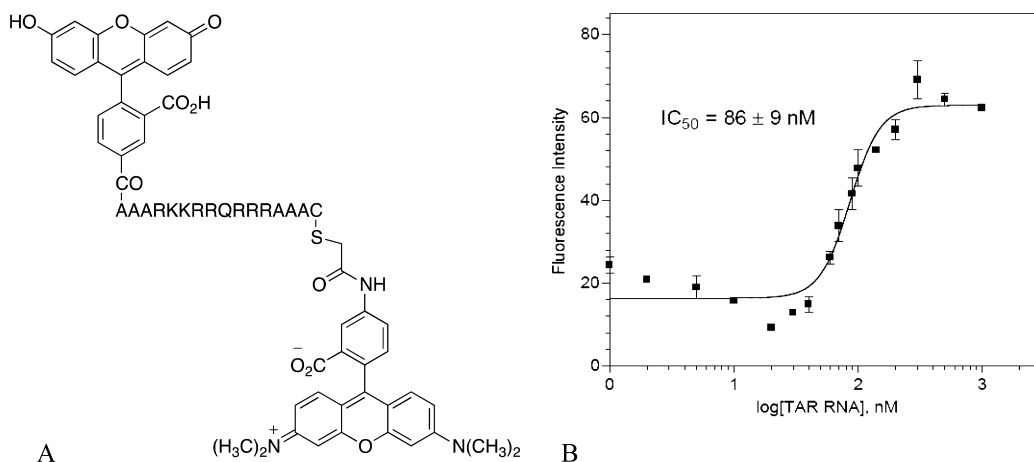


Figure 7. (A) Fluorescein-labeled Tat_{49–57} peptide used for the FRET-mediated fluoremetric competition binding assay. (B) Saturating binding curve of fluorescein-labeled Tat_{49–57} peptide with HIV TAR RNA at 25 °C. The binding affinity (IC₅₀) reported is the average of three to five individual measurements and was determined by fitting the experimental data to a sigmoidal dose–response nonlinear regression model via GraphPad Prism 4.0.

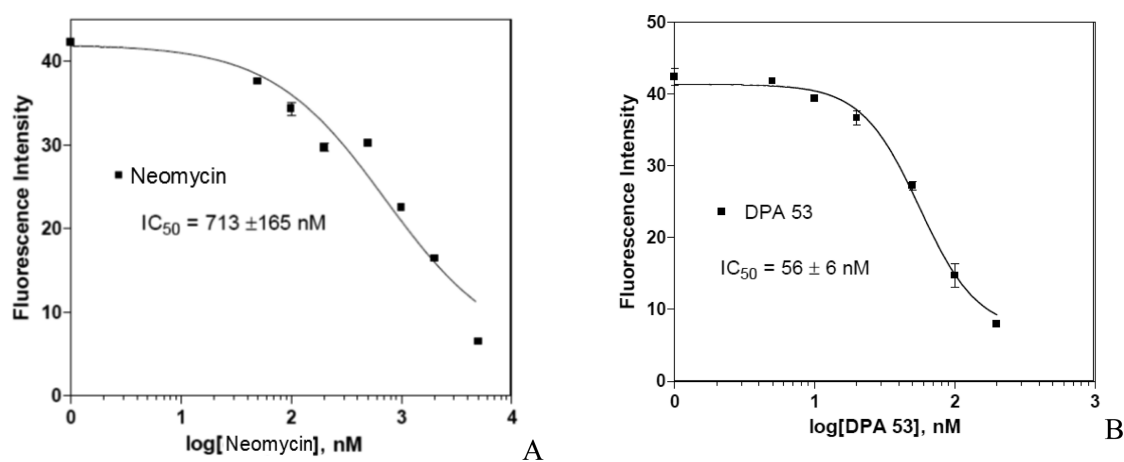


Figure 8. Determination of IC_{50} values using the FRET competition binding assay. Titration curves are shown for the IC_{50} values of (A) neomycin and (B) DPA53. The binding affinity (IC_{50}) values reported for each ligand are the averages of three to five individual measurements and were determined by fitting the experimental data to a sigmoidal dose–response nonlinear regression model via GraphPad Prism 4.0.

Table 7. IC_{50} Values of Ligands Determined by a FRET-Mediated Competition Binding Assay

Ligands	Linker length	Structure of the linker (-x-, from Scheme 1 and Scheme 2)	IC_{50} (nM)
Fluorescein-labeled-TAT peptide	NA	NA	86 ± 9
DPA51	7		77 ± 27
DPA52	7		60 ± 8
DPA65	7		47 ± 6
DPA53	8		56 ± 6
DPA54	8		58 ± 6
DPA55	10		80 ± 9
DPA56	10		59 ± 11
DPA58	16		61 ± 13
DPA60	20		67 ± 9
Neomycin	NA	NA	713 ± 165

(Figure 10). The results from both assays were comparable as observed from the trends in IC_{50} values as a function of linker length. The binding affinity of shorter and rigid linkers is higher and reflected in the lower IC_{50} value, as compared to the higher IC_{50} obtained with longer linkers. The lowest IC_{50} was dis-

played by DPA53 and DPA65 with HIV TAR RNA. Dimers DPA65 and DPA53 are the most rigid structures in the triazole library reported here. They have a phenyl ring between two neomycin units in addition to the two triazole rings leading to an extended aromatic system that enhances the linker rigidity of

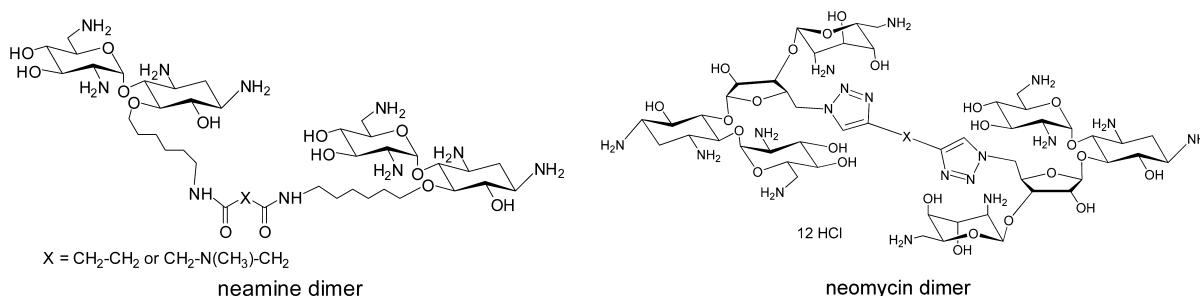


Figure 9. Chemical structure of neomycin and neamine dimers.

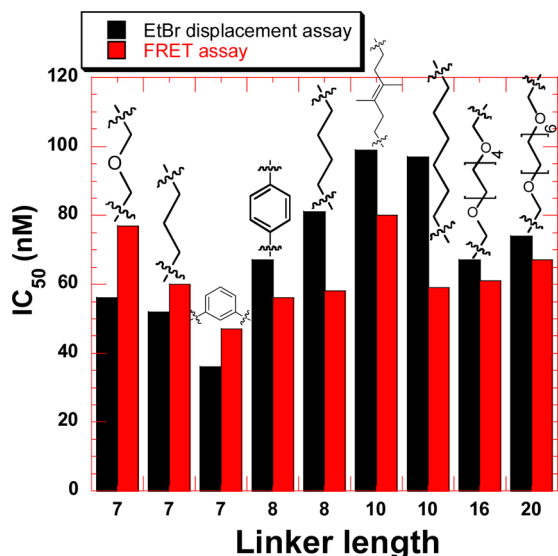


Figure 10. Bar graph showing the comparison of IC₅₀ values of neomycin dimers with HIV TAR RNA using a FRET-mediated competition binding assay and an ethidium bromide displacement assay.

these dimers in comparison to other more flexible dimers such as DPA52 and DPA54.

To investigate the specificity of the tight binders, we then studied the binding of DPA65 with a TAR mutant (tetraloop TAR), as shown in Figure 11. FID titrations were conducted between DPA65 and mutant TAR (Figure 12), and Scatchard analysis of the data yielded a K_d of $\sim 10^7$ M⁻¹. When compared to its affinity for wild-type HIV TAR RNA, DPA65 binds to mutant HIV TAR RNA with an affinity that is 1 order of magnitude lower, suggesting that linker length variations can lead to RNA binders with higher affinities and selectivity than monomeric aminoglycosides.

In Vitro Assay To Study the Effect of Neomycin Dimers in MT-2 Cells. An important step in the life cycle of HIV is the death of the infected cell population. The HIV envelope uses the CD4 cell as a receptor. The infection caused by HIV through CD4 results in an immense enhancement in the number of infected cells, including cell–cell fusion and cell death, a phenomenon called the cytopathic effect (CPE).⁶⁶ Neomycin dimers and neomycin were monitored for their ability to protect MT-2 cells from the cytopathic effect caused by HIV (Table 9). We first assessed toxicity against MT-2 cells, a CD4+, lymphoblastoid cell line. We utilized the highly restrictive definition of 5% cytotoxicity (CT₅), rather than the more commonly reported 50% cytotoxicity (CT₅₀), as HIV is an obligate intracellular parasite. Any toxic effects on the cell

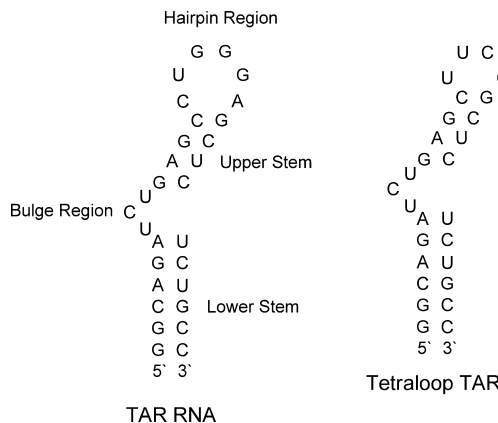


Figure 11. Structure of TAR RNA and mutant tetraloop TAR used in this study.

may manifest themselves as a perceived anti-HIV effect. CT₅ is a nontoxic concentration at which 95% of the cells are viable. The maximal concentrations of the neomycin conjugates used are listed in Table 9. For all compounds, this is the concentration of ligand at which no more than 5% cell death was observed (CT₅). For comparison, water was used as control.

We next assessed the anti-HIV activities of the compounds. This assay was performed in triplicate wells of a 96-well plate. It utilized Finter's neutral red dye, a vital dye, to assess the ability of any given antibody or compound to inhibit the HIV-induced cytopathic effect. As indicated in Table 8, neomycin dimers showed much improved protection from the cytopathic effect as opposed to neomycin and water (control). Neomycin dimer DPA52 showed little protection from the cytopathic effect, suggesting that minor variations in linker length can significantly affect the pharmacodynamic and/or pharmacokinetic properties of these ligands. Neomycin dimers DPA53–DPA56 showed 20–33% protection from the cytopathic effect in the concentration range of 4–17 μM. Overall, the compounds showed modest anti-HIV activity in this assay with a maximal 33% suppression of cell death.

We then confirmed the anti-HIV activity by two additional assays. These include the spread of HIV through culture, as measured by the immunofluorescence assay (IFA), and the release of reverse transcriptase (RT) into supernatant fluids. In this experiment, nontoxic concentrations of each of five neomycin dimers, with some anti-HIV activity (Table 8), were selected. We pretreated 500000 cells with each compound for 1 h. Next, cells were inoculated with approximately 50000 infectious particles of HIV_{NL4-3}. Infections were performed in triplicate. Every 2 days cells were collected and stained for HIV antigen synthesis. Culture supernatants were analyzed for RT release. As shown in Table 9, the compounds had a more robust effect on HIV antigen synthesis than was apparent in the

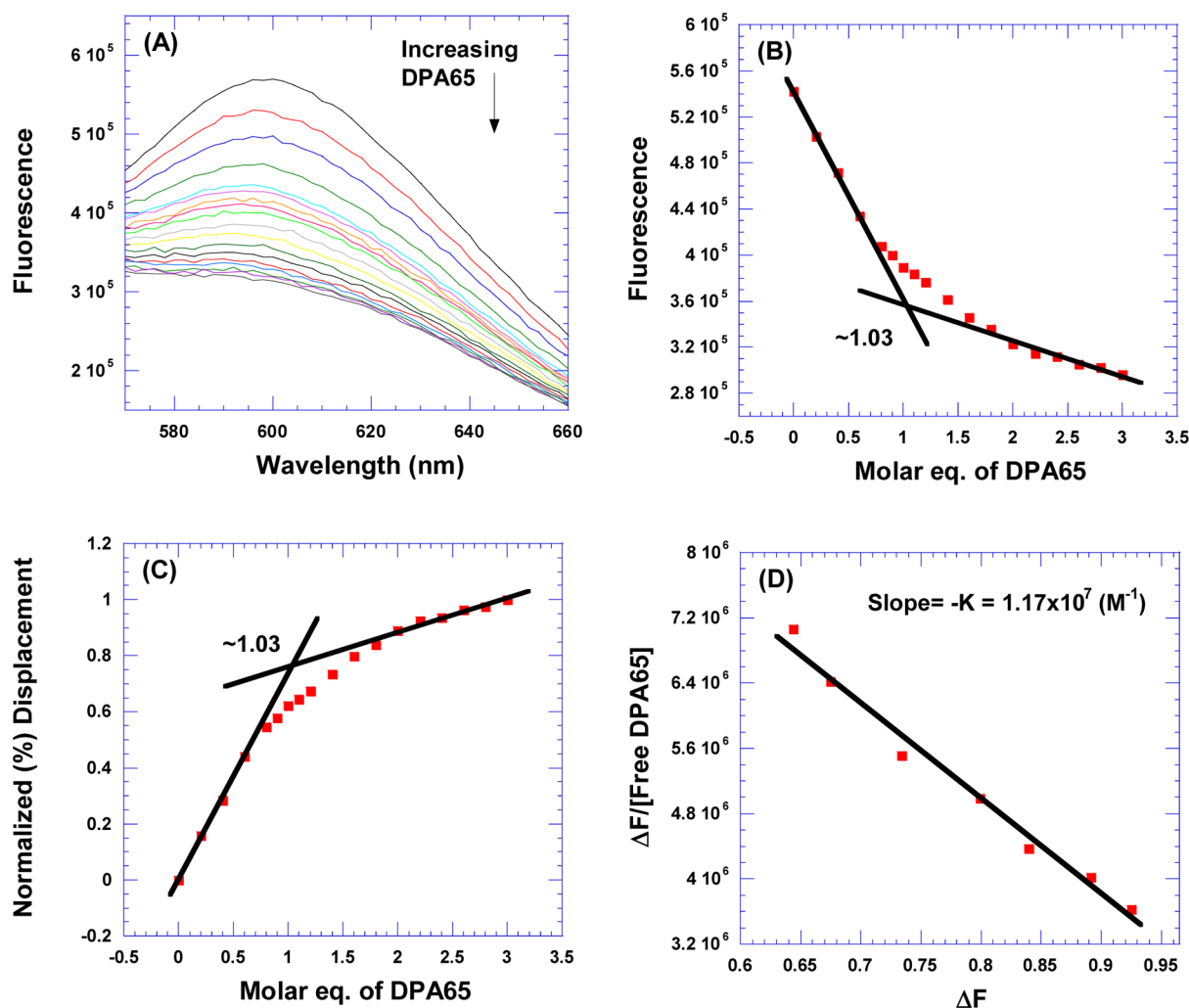


Figure 12. FID titration of DPA65 with a tetraloop TAR RNA mutant. (A) Raw fluorescence emission spectra in the presence of increasing concentrations of DPA65. (B) Decrease in fluorescence intensity (at 610 nm) of the tetraloop TAR RNA–EtBr complex with an increasing DPA65 concentration. (C) Plot between normalized fluorescence intensity (at 610 nm) of the tetraloop TAR RNA–EtBr complex as a function of DPA65 concentration. (D) Scatchard analysis of DPA65 with tetraloop TAR RNA. Buffer conditions: 100 mM KCl, 10 mM β C, 0.5 mM EDTA, pH 6.8. The tetraloop TAR RNA concentration was 200 nM/strand. The EtBr concentration was 5 μ M.

Table 8. Five Percent Toxicity Concentrations of Neomycin Dimers and Neomycin Showing the Maximal Protection Obtained from HIV Cytopathic Effects

	5% toxicity (μ M)	maximal protection [concentration achieved (μ M)]
neomycin	>206	9% (206)
DPAS2	>138	1% (9)
DPAS3	17	33% (8)
DPAS4	69	31% (17)
DPAS5	8	20% (4)
DPAS6	34	33% (17)
water	none	2%

cytopathicity assay. Indeed, several compounds inhibited HIV replication by as much as 70% (day 4).

The neomycin dimers inhibit HIV antigen synthesis effectively up to 4 days postinoculation. Neomycin dimers DPAS3, DPAS5, and DPAS6 inhibit HIV antigen synthesis from 60 to 70% up to the fourth day as opposed to other neomycin dimers. The virus control contains the infected cells and water solvent. Dimer DPAS3 has one of the highest affinities for HIV TAR

Table 9. Inhibition by Neomycin Dimers of HIV Antigen Synthesis in Treated Cells

	concn (μ M)	percent of HIV antigen synthesis		
		day 2	day 4	day 6
DPAS2	25	15	100	100
DPAS3	9	2	40	100
DPAS4	17	3–5	80	100
DPAS5	4	3–5	30	100
DPAS6	8	5–7	40	100
virus control	NA ^a	15	100	100

^aNot applicable.

RNA as borne out by the FRET-mediated competition binding assay, the ethidium bromide assay, and the UV thermal denaturation experiment.

Neomycin dimers also reduced the amount of reverse transcriptase (RT) released into the cell culture supernatant as opposed to the virus control.⁶⁷ HIV replication was suppressed by an even greater amount in this assay. For example, DPAS6 suppressed RT release by 90% at day 4 and at least 20% at day 6 (Table 10). A couple of important observations need to be

Table 10. Release of Reverse Transcriptase into the Culture Supernatant (counts per minute per milliliter)^a

	concn (μM)	day 2 (cpm/mL)	day 4 (cpm/mL)	day 6 (cpm/mL)
DPA52	25	21485 (4574)	347845 (10680)	268357 (57519)
DPA53	9	8880 (1373)	45539 (32831)	221445 (20678)
DPA54	17	14805 (1309)	165301 (22967)	427475 (49583)
DPA55	4	20072 (3748)	107933 (17963)	305277 (59913)
DPA56	8	15989 (2523)	105704 (15948)	412475 (19612)
virus control	NA ^b	46029 (6651)	928112 (126547)	1078741 (188673)

^aValues are means of triplicate infections, and values in parentheses are one standard deviation. ^bNot applicable.

noted. (1) All the neomycin dimers inhibit the release of RT. (2) Neomycin dimer DPA53 is the most effective among all the neomycin dimers studied, which is reflected by the maximal inhibition (Table 10) at moderate concentrations. (3) As opposed to the HIV antigen inhibition assay, neomycin dimers inhibit the release of RT even after 6 days.

These findings were somewhat surprising, as we do not usually see a significant anti-HIV effect in confirmatory assays that is stronger than the anti-HIV activity seen in the cytopathic effect assay (Table 8). A much more significant anti-HIV effect of neomycin dimers was seen in the confirmatory assays. Because DPA65 was one of the most potent binding agents, two separate experiments were performed to determine the anti-HIV activities of this compound. As with the other compounds, DPA65 was inactive to weakly active in the 96-well plate screening assay. When the anti-HIV properties of the compound as measured by the release of RT into the culture media were determined, they were highly reproducible over a period of months and over many replicates. The compound was tested three separate times, in triplicate each time. On day 2 post-inoculation, it protected cells by 40–67%. On day 4, it protected cells by 68–73%, and on day 6, it protected cells by 24–27%. The lower levels of protection on day 6 were due to lysis of the virus control infections on day 4, and thus, there was little additional release of virus into the culture media from day 4 to day 6. To ascertain whether the compounds were acting at Tat–TAR interactions within cells, we attempted to raise inhibitor-resistant virus by culturing HIV in increasing concentrations of neomycin dimers. We were not able to raise a resistant virus, indicating that the combination of anti-HIV activity with the likelihood of deleterious mutations within Tat or TAR precluded the selection of viable, inhibitor-resistant HIV. Nevertheless, the unusual finding of weaker activity against the HIV-induced cytopathic effect but a more potent inhibition of antigen synthesis is consistent with an effect on HIV transcription.

CONCLUSION

A series of neomycin dimers were synthesized via click chemistry in high yields. The dimers were then studied with HIV TAR RNA using various analytical techniques: UV thermal denaturation, CD titration, FID assay, a FRET-mediated competition binding assay, and in vitro cellular assays for HIV inhibition. There are a number of conclusions that can be drawn from the studies. (1) UV thermal denaturation studies show that neomycin dimers enhance the melting temperature of HIV TAR RNA up to 10.3 °C. The monomer neomycin does not show any effect on the thermal stabilization of HIV TAR RNA. The neomycin dimers with the shortest linker lengths displayed the highest thermal stabilization, which decreases with an increase in linker length. The concentration-dependent thermal denaturation studies indicate that the neomycin dimer binds

with a stoichiometry of 1:1 with HIV TAR RNA. (2) The CD spectra in the presence of a neomycin dimer suggest that it does not interact with the trinucleotide bulge region, which is the binding site of Tat protein. Additionally, neomycin dimer binding pushes the conformation of HIV TAR RNA away from an A-form. (3) The ethidium bromide displacement titration between neomycin dimers and HIV TAR RNA showed a binding stoichiometry of 1:1, validating the results from CD and UV thermal denaturation experiments. (4) Scatchard analysis of FID titrations results in a binding constant of 10^7 – 10^8 M⁻¹ between neomycin dimers and HIV TAR RNA depending on linker length. The trends in binding affinity obtained are similar to the trends in UV thermal denaturation stabilization. The neomycin dimers with shorter linker lengths show the highest affinity for HIV TAR RNA. (5) Salt-dependent studies show that despite the highly charged nature of the dimeric ligands, the major contributor to the free energy of binding comes from nonelectrolytic terms. (6) The FRET-mediated competition binding assay confirms the high affinity of neomycin dimers for HIV TAR RNA. The patterns of TAR RNA–dimer binding affinity are similar to those obtained from UV thermal denaturation and the FID assay. The binding affinity of neomycin is much weaker than those of all the neomycin dimers. (7) In vitro assays show that neomycin dimers are effective inhibitors of HIV. Some of the neomycin dimers effectively inhibit the release of reverse transcriptase at low concentration. Our studies outline the growing potential of click chemistry in efficiently generating multivalent ligands to improve binding of ligands to therapeutic targets. Further studies are ongoing to explore SAR of modified aminosugars, structural studies of binding, and the details of mechanisms of HIV inhibition by these dimers. These studies will be reported in due course.

ASSOCIATED CONTENT

Supporting Information

Characterization of triazole-linked neomycin dimers using click chemistry, UV thermal denaturation profiles, ethidium bromide displacement assay plots, FRET-mediated competition binding assay plots, and ethidium bromide displacement titration to determine the binding constant plots. This material is available free of charge via the Internet at <http://pubs.acs.org>.

AUTHOR INFORMATION

Corresponding Author

*Telephone: (864) 656-1106. Fax: (864) 656-6613. E-mail: dparya@clemsun.edu.

Notes

The authors declare no competing financial interest.

Funding

We thank the National Science Foundation (CHE/MCB-0134972) and the National Institutes of Health (R15CA125724) for financial support.

REFERENCES

- (1) Berkhout, B., and Jeang, K. T. (1989) Transactivation of human immunodeficiency virus type 1 is sequence specific for both the single-stranded bulge and loop of the trans-acting-responsive hairpin: A quantitative analysis. *J. Virol.* 63, 5501–5504.
- (2) Jones, K. A., and Peterlin, B. M. (1994) Control of Rna Initiation and Elongation at the Hiv-1 Promoter. *Annu. Rev. Biochem.* 63, 717–743.
- (3) Draper, D. E. (1995) Protein-RNA Recognition. *Annu. Rev. Biochem.* 64, 593–620.
- (4) Rosen, C. A., Sodroski, J. G., and Haseltine, W. A. (1985) The location of cis-acting regulatory sequences in the human T cell lymphotropic virus type III (HTLV-III/LAV) long terminal repeat. *Cell* 41, 813–823.
- (5) Muesing, M. A., Smith, D. H., and Capon, D. J. (1987) Regulation of mRNA accumulation by a human immunodeficiency virus trans-activator protein. *Cell* 48, 691–701.
- (6) Aboul-ela, F., Karn, J., and Varani, G. (1995) The Structure of the Human Immunodeficiency Virus Type-1 TAR RNA Reveals Principles of RNA Recognition by Tat Protein. *J. Mol. Biol.* 253, 313–332.
- (7) Rana, T. M., and Jeang, K. T. (1999) Biochemical and functional interactions between HIV-1 Tat protein and TAR RNA. *Arch. Biochem. Biophys.* 365, 175–185.
- (8) Hauber, J., and Cullen, B. R. (1988) Mutational analysis of the trans-activation-responsive region of the human immunodeficiency virus type I long terminal repeat. *J. Virol.* 62, 673–679.
- (9) Feng, S., and Holland, E. C. (1988) HIV-1 tat trans-activation requires the loop sequence within tar. *Nature* 334, 165–167.
- (10) Puglisi, J., Tan, R., Calnan, B., and Frankel, A. (1992) Williamson Conformation of the TAR RNA-arginine complex by NMR spectroscopy. *Science* 257, 76–80.
- (11) Thomas, J. R., and Hergenrother, P. J. (2008) Targeting RNA with Small Molecules. *Chem. Rev.* 108, 1171–1224.
- (12) Bailly, C., Colson, P., Houssier, C., and Hamy, F. (1996) The Binding Mode of Drugs to the TAR RNA of HIV-1 Studied by Electric Linear Dichroism. *Nucleic Acids Res.* 24, 1460–1464.
- (13) Ratmeyer, L. S., Vinayak, R., Zon, G., and Wilson, W. D. (1992) An ethidium analog that binds with high specificity to a base-bulged duplex from the TAR RNA region of the HIV-1 genome. *J. Med. Chem.* 35, 966–968.
- (14) Dassonneville, L., Hamy, F., Colson, P., Houssier, C., and Bailly, C. (1997) Binding of Hoechst 33258 to the TAR RNA of HIV-1. Recognition of a pyrimidine bulge-dependent structure. *Nucleic Acids Res.* 25, 4487–4492.
- (15) Lind, K. E., Du, Z., Fujinaga, K., Peterlin, B. M., and James, T. L. (2002) Structure-Based Computational Database Screening, In Vitro Assay, and NMR Assessment of Compounds that Target TAR RNA. *Chem. Biol.* 9, 185–193.
- (16) Tao, J., and Frankel, A. D. (1992) Specific binding of arginine to TAR RNA. *Proc. Natl. Acad. Sci. U.S.A.* 89, 2723–2726.
- (17) Hwang, S., Tamilarasu, N., Ryan, K., Huq, I., Richter, S., Still, W. C., and Rana, T. M. (1999) Inhibition of gene expression in human cells through small molecule-RNA interactions. *Proc. Natl. Acad. Sci. U.S.A.* 96, 12997–13002.
- (18) Athanassiou, Z., Patora, K., Dias, R. L. A., Moehle, K., Robinson, J. A., and Varani, G. (2007) Structure-Guided Peptidomimetic Design Leads to Nanomolar β -Hairpin Inhibitors of the Tat–TAR Interaction of Bovine Immunodeficiency Virus. *Biochemistry* 46, 741–751.
- (19) Mei, H., Mack, D. P., Galan, A. A., Halim, N. S., Heldsinger, A., Loo, J. A., Moreland, D. W., Sannes-Lowery, K. A., Sharmeen, L., Truong, H. N., and Czarnik, A. W. (1997) Discovery of selective, small-molecule inhibitors of RNA complexes. 1. The tat protein/TAR RNA complexes required for HIV-1 transcription. *Bioorg. Med. Chem.* 5, 1173–1184.
- (20) Raghunathan, D., Sánchez-Pedregal, V. M., Junker, J., Schwiegk, C., Kalesse, M., Kirschning, A., and Carlomagno, T. (2006) TAR-RNA recognition by a novel cyclic aminoglycoside analogue. *Nucleic Acids Res.* 34, 3599–3608.
- (21) Tor, Y. (2006) The ribosomal A-site as an inspiration for the design of RNA binders. *Biochimie* 88, 1045–1051.
- (22) Wang, S., Huber, P. W., Cui, M., Czarnik, A. W., and Mei, H. (1998) Binding of Neomycin to the TAR Element of HIV-1 RNA Induces Dissociation of Tat Protein by an Allosteric Mechanism. *Biochemistry* 37, 5549–5557.
- (23) Charles, I., Xi, H., and Arya, D. P. (2007) Sequence-specific targeting of RNA with an oligonucleotide-neomycin conjugate. *Bioconjugate Chem.* 18, 160–169.
- (24) Shaw, N. N., Xi, H., and Arya, D. P. (2008) Molecular recognition of a DNA:RNA hybrid: Sub-nanomolar binding by a neomycin-methidium conjugate. *Bioorg. Med. Chem. Lett.* 18, 4142–4145.
- (25) Shaw, N. N., and Arya, D. P. (2008) Recognition of the unique structure of DNA:RNA hybrids. *Biochimie* 90, 1026–1039.
- (26) Xi, H., Gray, D., Kumar, S., and Arya, D. P. (2009) Molecular recognition of single-stranded RNA: Neomycin binding to poly(A). *FEBS Lett.* 583, 2269–2275.
- (27) Arya, D. P. (2011) New approaches toward recognition of nucleic acid triple helices. *Acc. Chem. Res.* 44, 134–146.
- (28) Xi, H., Davis, E., Ranjan, N., Xue, L., Hyde-Volpe, D., and Arya, D. P. (2011) Thermodynamics of Nucleic Acid “Shape Readout” by an Aminosugar. *Biochemistry* 50, 9088–9113.
- (29) Xue, L., Ranjan, N., and Arya, D. P. (2011) Synthesis and spectroscopic studies of the aminoglycoside (Neomycin)-perylene conjugate binding to human telomeric DNA. *Biochemistry* 50, 2838–2849.
- (30) Ranjan, N., Andreasen, K. F., Kumar, S., Hyde-Volpe, D., and Arya, D. P. (2010) Aminoglycoside Binding to *Oxytricha nova* Telomeric DNA. *Biochemistry* 49, 9891–9903.
- (31) Willis, B., and Arya, D. P. (2010) Triple recognition of B-DNA by a neomycin-Hoechst 33258-pyrene conjugate. *Biochemistry* 49, 452–469.
- (32) Xi, H., Kumar, S., Dosen-Micovic, L., and Arya, D. P. (2010) Calorimetric and spectroscopic studies of aminoglycoside binding to AT-rich DNA triple helices. *Biochimie* 92, 514–529.
- (33) Xue, L., Xi, H., Kumar, S., Gray, D., Davis, E., Hamilton, P., Skriba, M., and Arya, D. P. (2010) Probing the recognition surface of a DNA triplex: Binding studies with intercalator-neomycin conjugates. *Biochemistry* 49, 5540–5552.
- (34) Willis, B., and Arya, D. P. (2009) Triple Recognition of B-DNA. *Bioorg. Med. Chem. Lett.* 19, 4974–4979.
- (35) Willis, B., and Arya, D. P. (2006) Major groove recognition of DNA by carbohydrates. *Curr. Org. Chem.* 10, 663–673.
- (36) Willis, B., and Arya, D. P. (2006) Recognition of B-DNA by Neomycin-Hoechst 33258 Conjugates. *Biochemistry* 45, 10217–10232.
- (37) Willis, B., and Arya, D. P. (2006) An expanding view of aminoglycoside-nucleic acid recognition. *Adv. Carbohydr. Chem. Biochem.* 60, 251–302.
- (38) Arya, D. P. (2005) Aminoglycoside-Nucleic Acid Interactions: The Case for Neomycin. *Top. Curr. Chem.* 253, 149–178.
- (39) Xi, H., and Arya, D. P. (2005) Recognition of triple helical nucleic acids by aminoglycosides. *Curr. Med. Chem.: Anti-Cancer Agents* 5, 327–338.
- (40) Arya, D. P., Xue, L., and Willis, B. (2003) Aminoglycoside (Neomycin) Preference Is for A-Form Nucleic Acids, Not Just RNA: Results from a Competition Dialysis Study. *J. Am. Chem. Soc.* 125, 10148–10149.
- (41) Arya, D. P., Micovic, L., Charles, I., Coffee, R. L. Jr., Willis, B., and Xue, L. (2003) Neomycin Binding to Watson-Hoogsteen (W-H) DNA Triplex Groove: A Model. *J. Am. Chem. Soc.* 125, 3733–3744.

- (42) Arya, D. P., and Willis, B. (2003) Reaching into the major groove of B-DNA: Synthesis and nucleic acid binding of a neomycin-Hoechst 33258 conjugate. *J. Am. Chem. Soc.* 125, 12398–12399.
- (43) Arya, D. P., Xue, L., and Tennant, P. (2003) Combining the best in triplex recognition: Synthesis and nucleic acid binding of a BQQ-neomycin conjugate. *J. Am. Chem. Soc.* 125, 8070–8071.
- (44) Xue, L., Charles, I., and Arya, D. P. (2002) Pyrene-neomycin conjugate: Dual recognition of a DNA triple helix. *Chem. Commun.* 1, 70–71.
- (45) Hamilton, P. L., and Arya, D. P. (2012) Natural product DNA major groove binders. *Nat. Prod. Rep.* 29, 134–143.
- (46) Arya, D. P., and Coffee, R. L. Jr. (2000) DNA Triple Helix Stabilization by Aminoglycoside Antibiotics. *Bioorg. Med. Chem. Lett.* 10, 1897–1899.
- (47) Arya, D. P., Coffee, R. L. Jr., Willis, B., and Abramovitch, A. I. (2001) Aminoglycoside-nucleic acid interactions: Remarkable stabilization of DNA and RNA triple helices by neomycin. *J. Am. Chem. Soc.* 123, 5385–5395.
- (48) Arya, D. P., Coffee, R. L. Jr., and Charles, I. (2001) Neomycin-Induced Hybrid Triplex Formation. *J. Am. Chem. Soc.* 123, 11093–11094.
- (49) Wang, H., and Tor, Y. (1997) Dimeric aminoglycosides: Design, synthesis and RNA binding. *Bioorg. Med. Chem. Lett.* 7, 1951–1956.
- (50) Michael, K., Wang, H., and Tor, Y. (1999) Enhanced RNA binding of dimerized aminoglycosides. *Bioorg. Med. Chem.* 7, 1361–1371.
- (51) Riguet, E., Desire, J., Boden, O., Ludwig, V., Gobel, M., Bailly, C., and Decout, J. L. (2005) Neamine dimers targeting the HIV-1 TAR RNA. *Bioorg. Med. Chem. Lett.* 15, 4651–4655.
- (52) Sannes-Lowery, K. A., Mei, H., and Loo, J. A. (1999) Studying aminoglycoside antibiotic binding to HIV-1 TAR RNA by electrospray ionization mass spectrometry. *Int. J. Mass Spectrom.* 193, 115–122.
- (53) Matsumoto, C., Hamasaki, K., Mihara, H., and Ueno, A. (2000) A high-throughput screening utilizing intramolecular fluorescence resonance energy transfer for the discovery of the molecules that bind HIV-1 TAR RNA specifically. *Bioorg. Med. Chem. Lett.* 10, 1857–1861.
- (54) Kolb, H. C., and Sharpless, K. B. (2003) The growing impact of click chemistry on drug discovery. *Drug Discovery Today* 8, 1128–1137.
- (55) Kolb, H. C., Finn, M. G., and Sharpless, K. B. (2001) Click Chemistry: Diverse Chemical Function from a Few Good Reactions. *Angew. Chem., Int. Ed.* 40, 2004–2021.
- (56) Rostovtsev, V. V., Green, L. G., Fokin, V. V., and Sharpless, K. B. (2002) A stepwise Huisgen cycloaddition process: Copper(I)-catalyzed regioselective ligation of azides and terminal alkynes. *Angew. Chem., Int. Ed.* 41, 2596.
- (57) Kumar, S., and Arya, D. P. (2011) Recognition of HIV TAR RNA by triazole linked neomycin dimers. *Bioorg. Med. Chem. Lett.* 21, 4788–4792.
- (58) Kumar, S., Xue, L., and Arya, D. P. (2011) Neomycin-Neomycin Dimer: An All-Carbohydrate Scaffold with High Affinity for AT-Rich DNA Duplexes. *J. Am. Chem. Soc.* 133, 7361–7375.
- (59) Arya, D. P., Coffee, R. L., and Xue, L. (2004) From triplex to B-form duplex stabilization: Reversal of target selectivity by aminoglycoside dimers. *Bioorg. Med. Chem. Lett.* 14, 4643–4646.
- (60) Charles, I., Xue, L., and Arya, D. P. (2002) Synthesis of aminoglycoside-DNA conjugates. *Bioorg. Med. Chem. Lett.* 12, 1259–1262.
- (61) Charles, I., and Arya, D. P. (2005) Synthesis of neomycin-DNA/peptide nucleic acid conjugates. *J. Carbohydr. Chem.* 24, 145–160.
- (62) Suryawanshi, H., Sabharwal, H., and Maiti, S. (2010) Thermodynamics of Peptide-RNA Recognition: The Binding of a Tat Peptide to TAR RNA. *J. Phys. Chem. B* 114, 11155–11163.
- (63) Boger, D. L., Fink, B. E., Brunette, S. R., Tse, W. C., and Hedrick, M. P. (2001) A Simple, High-Resolution Method for Establishing DNA Binding Affinity and Sequence Selectivity. *J. Am. Chem. Soc.* 123, 5878–5891.
- (64) Record, M. T. Jr., Anderson, C. F., and Lohman, T. M. (1978) Thermodynamic analysis of ion effects on the binding and conformational equilibria of proteins and nucleic acids: The roles of ion association or release, screening, and ion effects on water activity. *Q. Rev. Biophys.* 11, 103–178.
- (65) Spolar, R. S., Livingstone, J. R., and Record, M. T. (1992) Use of liquid hydrocarbon and amide transfer data to estimate contributions to thermodynamic functions of protein folding from the removal of nonpolar and polar surface from water. *Biochemistry* 31, 3947–3955.
- (66) Leonard, R., Zagury, D., Desportes, I., Bernard, J., Zagury, J. F., and Gallo, R. C. (1988) Cytopathic effect of human immunodeficiency virus in T4 cells is linked to the last stage of virus infection. *Proc. Natl. Acad. Sci. U.S.A.* 85, 3570–3574.
- (67) Robinson, W. E., Montefiori, D. C., Gillespie, D. H., and Mitchell, W. M. (1989) Complement-Mediated, Antibody-Dependent Enhancement of HIV-1 Infection in Vitro Is Characterized by Increased Protein and RNA Syntheses and Infectious Virus Release. *JAIDS, J. Acquired Immune Defic. Syndr.* 2, 33–42.